Molecular Dynamics Study of A Water Soluble, Upper Critical Solution Temperature Polymer

by

Yang Zhou

A thesis submitted in partial fulfillment of the requirements for the degree of

Master of Science

in
Chemical Engineering

Department of Chemical and Materials Engineering
University of Alberta

Abstract

The phase behavior of a water-soluble, non-ionic polymer namely poly(N-acryloyl glycinamide) (poly(NAGA)) was studied by molecular dynamics simulation. PolyNAGA is experimentally observed to exhibit the so-called upper critical solution temperature (UCST) phase behavior in water. This is atypical as majority of water-soluble, non-ionic polymers exhibit the opposite phase behavior – the lower critical solution temperature (LCST) phase behavior. In this work, the conformation of polyNAGA in water, which is quantified by its radius of gyration, was used to infer the solubility behavior of the polymer. In particular, radii of gyration of polyNAGA in water over the temperature range that the polymer is observed to exhibit the UCST behavior were calculated from MD simulations. It is worth noting that a polymer that is soluble in a solvent tends to exhibit larger radius of gyration. Situations involving single and multiple chains in water were examined. Different partial atomic charge assignment methods, force fields and water models were used to determine whether the UCST phenomenon could be reproduced. Two single chain models, one with 10 repeating units while the other 30 repeating units along with 2,109 and 6,982 water molecules were used to build the corresponding polyNAGA solutions. Respective concentrations of the polyNAGA solutions were 3.3 and 2.9 wt%. The multiple chain model contained 5 polyNAGA chains each with 30 repeating units and 16,273 water molecules (6.2 wt% polyNAGA). The COMPASS, OPLS-AA, charge equilibration (QEq), and Gasteiger charges were assigned to all the atoms in polyNAGA. The dispersion interactions were described by the OPLS-AA and AMBER force fields. TIP4P, TIP3P and

SPC/E water models were used. It was found that for the solution model containing a single polyNAGA chain with 10 repeating units, use of the OPLS-AA force field along with the Gasteiger charges and TIP4P water model yielded an inverse temperature dependence of the radius of gyration of polyNAGA, suggesting the UCST phase behavior. In particular, the radius of gyration of polyNAGA was determined to be 0.65 nm $\pm$ 0.04 nm at 360 K while that at 280 K was 0.56 nm $\pm$ 0.01 nm. The number of hydrogen bonds between polyNAGA and water decreased with increasing temperature. The number of intra-molecular hydrogen bonds of polyNAGA was also found to be decreasing with increasing temperature. For the single polyNAGA chain with 30 repeating units, no combinations of the partial atomic charges, force field and water model yielded results that would suggest the experimentally observed phase behavior of polyNAGA. However, for the model containing multiple polyNAGA chains each with 30 repeating units, the use of OPLS-AA force field along with the Gasteiger charges and SPC/E water model led to results that suggested the UCST behavior of polyNAGA solution. Our data showed that the UCST behavior of polyNAGA was attributed to the decrease in intramolecular hydrogen bonds as temperature increased.

Dedicated to my parents, Youxing Zhou and Hehua Yang . . .

Acknowledgements

I would like to express my very great appreciation to my supervisor, Dr. Phillip Choi, who has the attitude and the substance of a genius. He continually and convincingly conveyed a spirit of adventure in regard to research. He is an excellent teacher for both my academic study and my life in general. Without his guidance and persistent help this dissertation would not have been possible. During my research process, I met so many difficulties, he was the individual who gave me the faith and encouraged me to move forward. In addition to the guidance for the research and study, Dr. Choi behaved like a father who always shared the interesting things with me and taught me to be a better man in life.

I would also like to offer my special thanks to Dr. Diwen Zhou, who was in the same group with me. He taught me the fundamental knowledge of molecular simulation and gave me lots of suggestions when I encountered problems. He was like a big brother who helped me when I was in trouble.

My special thanks are extended to Abolfazl Noorjahan, who is a doctoral student in Dr. Choi's group, for his kindness help. He is an energetic researcher who possesses a considerable amount of knowledge. He gave me lots of solutions when I met so many unexpected problems of the simulation software GROMACS.

My special thanks also go to Negin Razavilar and Jan Ulric Garcia, for helping me on learning GROMACS and programming.

I am particularly grateful for the support and good times that my friends have provided to me, they always stand up for me and help me whenever I need it.

The funding from the Natural Sciences and Engineering Research Council of Canada (NSERC) and the WestGrid and Compute/Calcul Canada for providing the computing resource were greatly appreciated.

To my family, I am grateful for their continual faith and support. Without them, I could not have pursued my dream of studying in Canada.

Contents

List of Figures

List of Tables

Abbreviations

UCST	**U**pper **C**ritical **S**olution **T**emperature
LCST	**L**ower **C**ritical **S**olution **T**emperature
MD	**M**olecular **D**ynamics
OPLS-AA	**O**ptimized **P**otentials for **L**iquid **S**imulations **A**ll **A**tom
SPC/E	**S**ingle **P**oint **C**harge / **E**xtended

Physical Constants

Avogadro's Constant	N_A	=	$6.022\ 141\ 29 \times 10^{23}$ mol^{-1}
The vacuum permittivity	ϵ_0	=	$8.854\ 187\ 82 \times 10^{-12}\ Fm^{-1}$
Elementary charge	e	=	$1.602\ 176\ 57 \times 10^{-19}\ Coulombs$

Symbols

m	mass	kg
t	time	s
F	Force	Newton
P	Potential	$N * m$
E	Energy	J
q	Charge	C
Q	Charge	C
G	Gibbs free energy	J
T	temperature	K
r	position	m
v	velocity	m/s
$\emptyset$	volume fraction	
A	Lennard-Jones parameter with r^{12}	
C	Lennard-Jones parameter with r^6	
θ	bond angle	degree
δ	charge bond increment	
K_r	bond parameter	
K_θ	angle parameter	
V	dihedral parameter	
ϵ_0	the vacuum permittivity	Fm^{-1}
λ	electronegativity	
D	electronegativity difference	

Chapter 1

Motivation and introduction

Thermo-responsive polymers have been the subject of intensive research in academic and industry over the past few decades. Water-soluble, thermo-responsive polymers have drawn significant attention because water is the most common solvent for many inorganic and organic polymers [1]. Among the thermo-responsive properties of interest, the change in the solubility of the polymers in water due to the temperature change is the most interesting one. In general, the phase behavior of such polymers is classified into two types – phase separation upon heating and phase separation upon cooling, respectively. In practice, one of the most frequently used water-soluble, thermo-responsive polymers that exhibits phase separation upon heating (the so-called lower critical solution temperature (LCST) behavior) is poly(N-isopropylacrylamide) (PNiPAAm). It should be noted that polymers that dissolve in organic solvents tend to exhibit the opposite solubility behavior (i.e., phase separation upon cooling or the so-called upper critical solution temperature (UCST) behavior).

The current project has focused on the study of a water-soluble, non-ionic polymer that exhibits the UCST behavior. The motivation behind the research is to understand the molecular mechanism that is responsible for its solubility behavior. Such understanding would allow us to design water-soluble, UCST polymers that can be used in a variety of applications. For example, such polymers have the potential to be used as flocculants in the oil sands tailing treatment process. It is conceivable that the phase behavior is mainly determined by the electrostatic interactions and hydrogen bonds. In this work, we used molecular dynamics simulation along with different partial atomic charge assignment methods, force fields and water models. The water-soluble, nonionic homopolymer of interest was poly(N-acryloyl glycinamide) (polyNAGA) that is experimentally observed to exhibit the UCST behavior in water.

1.1 literature review

As mentioned, water-soluble polymers are rare. Within them, most water-soluble polymers exhibit LCST behavior while all polymers that dissolve in organic solvents exhibit UCST behavior. There are only a few water-soluble polymers that show UCST behavior. There are a considerable amount of references on the solubility behavior of water-soluble polymers exhibiting the LCST behavior [2–5]. Work on water-soluble, UCST polymers is scanty. However, Seuring et al. published a review paper on water-soluble polymers that exhibit the upper critical solution temperatures in aqueous solutions [1].

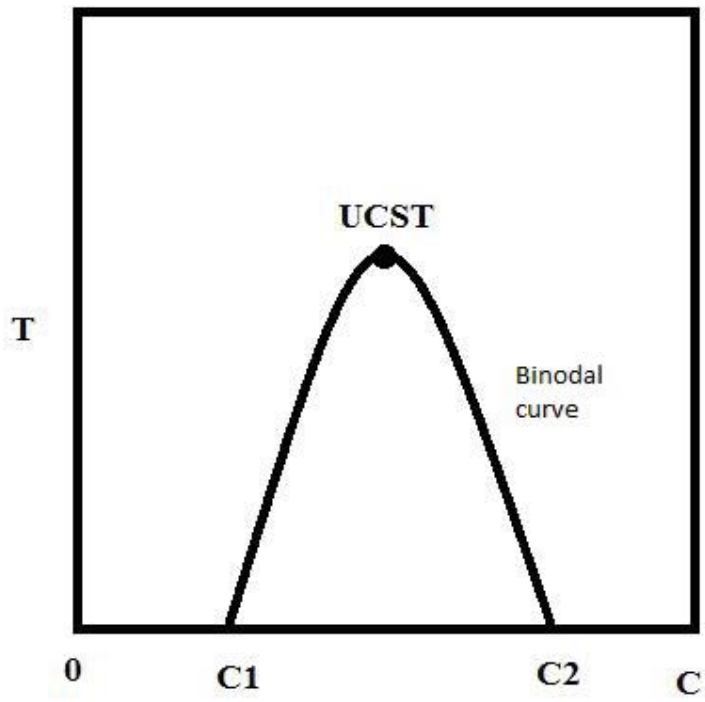

FIGURE 1.1: A schematic phase diagram of a UCST polymer solution

1.1.1 Phase behavior of polymer solution

In general, for a polymer exhibiting either UCST or LCST phase behavior, the polymer is miscible with the solvent in all proportions above the UCST or below the LCST, respectively. The phase transition is often shown using an isobaric phase diagram where the temperature is plotted against the solute concentration as shown schematically in Figure 1.1. In this particular case, the solute is immiscible with the solvent in the region enclosed by the phase boundary line called binodal. In particular, the solute and solvent are miscible at all concentrations above the UCST.

To understand phase behavior, one needs to consider the Gibbs free energy of mixing. The solution needs to exhibit a negative change on the Gibbs free energy of mixing and a positive second derivative of the Gibbs free energy of mixing with respect to the concentration. According to the Flory-Huggins solution model, the Gibbs free energy change of mixing for a binary polymer solution is given by the following expression [6–8].

$$\Delta G_m = RT[\, n_1 \ln \phi_1 + n_2 \ln \phi_2 + n_1 \phi_2 \chi_{12} \,] \tag{1.1}$$

In the above equation, n_i is the number of moles of component i and ϕ_i is the volume fraction of component i. The parameter χ_{12} is used to account for the energy of mixing two components. R is the gas constant and T is the absolute temperature. The volume fraction is used to account for the difference in the sizes of the components.

Another important fact of polymer solutions is that some polymers have high glass transition temperature that will lead to vitrify in the range of high polymer concentration. The intersection of the Tg curve with the binodal is called Berghmans points [1].

In practice, the cloud point is used to characterize the phase behavior of polymer solutions. The cloud point of a solution is the temperature at which the solute is no longer soluble in the solvent, precipitating as a second phase giving the liquid a cloudy appearance. In practice, the cloud point is determined by characterizing the turbidity of the solution.

1.1.2 Characterization of phase transition

Usually, the turbidity meter is used to measure the cloud point of a solution [9]. It is the easiest and most convenient method to determine the phase diagram of a given polymer solution. The cloud point is different from the concept of the phase boundary defined by LCST and UCST. The LCST or UCST is the minimum or the maximum temperature on the binodal curve at a distinct polymer concentration. But the cloud point is the temperature when the solution at a given concentration becomes turbid. Usually, the cloud point determined by heating a polymer solution is different from that by cooling the same polymer solution, referred to as hysteresis [1]. The hysteresis is caused by the polymer chain mobility in the solution. For example, the hysteresis of polyNAGA can be as large as 10 K in water.

1.1.3 UCST behavior caused by ionic interactions

Polymers containing ionic groups are among the most important classes of macromolecules. Ionic polymers are mainly divided into two groups, polyelectrolytes and polyzwitterions [10]. Only few of them exhibit the UCST behavior in water. Mary et al. investigated the water solubility of sufobetaine polyzwitterions [11]. These polymers have both positive ammonium and negative sulfonate charges on each monomer. As a result, they exhibit upper critical solution temperature (UCST) over the temperature range of 0 - 100 °C. The ionic polymers are sensitive to the ionic concentration. Koberle et al. did some work on the interaction of a zwitterionic polysoap and its cationic analog with inorganic salt [12]. They found

that the aqueous solution properties of such polymers are strongly influenced by added salts. The addition of salt can result in antipolyelectrolyte behavior. It is well known that different salts and different concentration have different solubility promotion abilities. McCormick et al. published a paper to discuss the solution properties and synthesis of zwitterionic polymers [10]. The formation of intra and inter-chain ionic interaction will lead to ionically cross-link network in the water. Therefore, most of previous studies on water soluble, UCST polymers focused on ionic polymers at low, controlled salt concentration in order to get turbidity transition phenomenon.

1.1.4 UCST behavior caused by hydrogen bonds

Poly(N-acryloylglycinamide) (PolyNAGA) is the most studied polymer with the UCST behavior that is attributed to the thermally reversible hydrogen bonds (H-bonds) [13]. Seuring et al. showed that non-ionic homo and copolymers with H-donor and H-acceptor units are also able to show the UCST behavior in water [14]. The polymers were synthesized by free radical copolymerization. Since such polymers had H-donors and H-acceptors, they could form inter-chain and intra-chain hydrogen bonds. Although polyNAGA was synthesized a while ago, its UCST behavior was not found until recent time. Since the polymer synthesized in early days contained ionic groups and the side chains were hydrolysized, the polymer did not exhibit the UCST behavior. Liu et al. used a controlled radical polymerization process to synthesize polyNAGA [9]. In order to get rid of the ionic pollution, they used nonionic initiator and nonionic chain transfer agent.

The experiment was conducted without air and water in order to prevent the production from hydrolysis. In this way, they observed the UCST of polyNAGA in water based upon cloud point measurements. Later, Seuring et al. regarded the polyNAGA as a water soluble, UCST polymer that has a high potential to be used in a variety applications in the future [1]. Tamai et al. compared different influence of hydrogen bonds to the poly(vinyl alcohol)(PVA), PVME and PNiPAAm [15, 16].

1.1.5 Molecular simulation

The simulation of water soluble, UCST polymers are still in early stage while the LCST polymers (e.g., PNiPAAm) have been intensively studied both theoretically and experimentally. Alaghemandi and Spohr used molecular dynamics simulation to investigate the phase behavior of poly(N-isopropylacrylamide) [17]. Du and Qian also investigated the hydrophilic to hydrophobic transition of PNiPAM-co-PEGMA with classical molecular dynamics simulation in relation to its LCST [18]. Only a few studies of water soluble, UCST polymers using molecular simulation have been reported. Srikant et al. used molecular dynamics simulation to investigate poly (acrylic acid) at infinite dilute condition in water. Molecular dynamics simulation with explicit solvent molecules was done and the effect of degree of ionization of poly(acrylic acid), a factor that determines the UCST behavior, was also investigated [19]. Gangemi et al. performed a 75 ns molecular dynamics simulation of NIPAAm oligomer containing 26 repeating units at two temperatures and compared the conformation of the polymer chains to that of experiment [20]. Netz and Dorfmuller investigated the interaction between polycarylamide and SPC/E

water molecules in the polymer solutions [21]. Simmons and Sanchez developed a scaled particle theory for the coil to globule transition of the PNIPAAm polymer chains [22]. Nonetheless, molecular dynamics simulation of water soluble, UCST polymers is rare. In fact, no one has done molecular dynamics simulation on poly-NAGA. This is the major thrust of the present work. It is our attempt to identify the molecular mechanism that is responsible for its UCST behavior. Figure 1.2

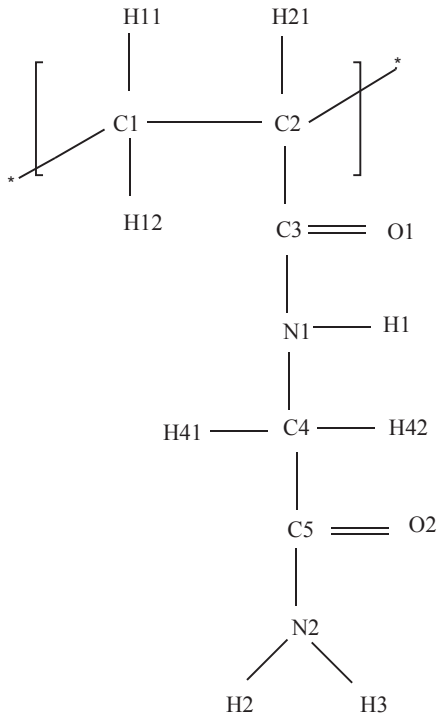

FIGURE 1.2: The repeating unit of polyNAGA

shows the repeating unit of polyNAGA.

1.2 Key objectives

One of the main objectives was to study the molecular mechanism that is responsible for the UCST behavior of polyNAGA. We used single chain and multiple

chains models over a wide range of temperatures. Compared to the well-studied example of PNiPAAm, which exhibits a sharp coil to globule transition in water at LCST, the polyNAGA exhibits an opposite behavior. The present work attempts to explain why some polymers like PNiPAAm have LCST, but some polymers like polyNAGA have UCST. Another purpose is to study how the intra-chain and inter-chain interactions contribute to the phase change of the system. According to the literature, the cloud point of 1.0 wt% poly(NAGA) in pure water is 22-23 °C [1].

1.3 Methodology

1.3.1 Single PolyNAGA chain in water

All molecular dynamics simulations were performed using the commericial software Materials Studio from Accelrys and an open source molecular dynamics code GROMACS. The polyNAGA models used contained either 10 or 30 monomer units. Each model was subjected to the three-dimensional periodic boundary conditions. The initial structures were energy minimized. In the regards, we used COMPASS force field to describe the polymer [23]. We used Materials Studio to build the systems and GROMACS to perform the molecular dynamcis simulation. All simulations were carried out at a constant pressure of 1 atm. Different temperatures were used in an attempt to capture the transition temperatures. Upon completion of the simulations, radii of gyration, numbers of hydrogen bonds of individual chains were analyzed to discern the temperature effect [18]. There exist

different types of hydrogen bonds in the systems of interest including polymer-polymer, polymer-water, and water-water. Regarding the polymer-polymer hydrogen bonds, there are inter and intra-chain types. Obviously, numbers of different types of hydrogen bonds vary with temperature, thereby leading to phase transition. For UCST polymers, it is expected that changing the temperature will alter the balance of the number of hydrogen bonds between water and polymer and those between polymers that lead to the observed phase behavior.

1.3.2 Multiple PolyNAGA chains in water

We also performed simulations using multiple chain (5 chains) models. In these simulations, each polyNAGA chian contained 30 monomer units. Once again, we used COMPASS force field for the polyNAGA chains for energy minimization. The simulations were done at a constant pressure of 1 atm. A data analysis strategy similar to that used for the single chain model was used.

1.4 Molecular dynamics simulation

Simulation parameters are always the most important part of running a proper simulation. The correct parameters are the keys to make sure that experiment observation can be reproduced. This section aims at explaining several simulation parameters and giving reasons why we choose specific parameters.

1.4.1 Newton's second law

MD simulation solves Newton's equations of motion of the atom (particle) of interest:

$$m_i \frac{\partial^2 r_i}{\partial t^2} = F_i, i = 1...N \tag{1.2}$$

The forces are the negative derivatives of a potential function P:

$$F_i = -\frac{\partial P}{\partial r_i} \tag{1.3}$$

The leap-frog algorithm was used for integrating Newton's equations of motion. GROMACS defaults this algorithm for the integration of the equations of motion. The leap-frog algorithm uses positions r and velocity v for integrating the equation of motion.

$$v(t + \frac{1}{2}\triangle t) = v(t - \frac{1}{2}\triangle t) + \frac{\triangle t}{m} F(t) \tag{1.4}$$

$$r(t + \triangle t) = r(t) + \triangle t v(t + \frac{1}{2}\triangle t) \tag{1.5}$$

In such an integrator, the motion of system is recorded. The equations of motion can be modified by the factor from temperature coupling and pressure coupling.

1.4.2 Force fields

In this research, all-atoms force fields were considered since the hydrogen bond interaction was the most important part. The main purpose of the research is to investigate the intermolecular interaction of the polymer-water system. The

OPLS-AA force field and AMBER force field were used previously for bio molecules containing carbon, nitrogen, oxygen and hydrogen. We felt justified to use the force fields to describe polyNAGA as it also contains similar atoms. Further validation of the force fields was not needed. The hydrogen bond is the electromagnetic attractive interaction between polar molecules. So in this case, the hydrogen on the polymer chains or on the water is very important to reproduce the UCST phenomenon. The OPLS (Optimized Potential for Liquid Simulations) force field as an all-atom force field is suitable for our purpose. The force field is previously designed in the computer simulation of proteins in their native environment. The nonbonded interactions are represented by the Coulomb and Lennard-Jones terms below.

$$\mathrm{E}_{ab} = \sum_{i}^{a} \sum_{j}^{b} \left(\frac{q_i q_j \mathrm{e}^2}{r_{ij}} + \frac{A_{ij}}{r_{ij}^{12}} - \frac{C_{ij}}{r_{ij}^{6}} \right) \tag{1.6}$$

Both A and C are the lennard-Jones parameters. Standard combing rules are used such that $A_{ij} = (A_{ii}A_{jj})^{1/2}$ and $C_{ij} = (C_{ii}C_{jj})^{1/2}$. The energy for bond stretching and angle bending are:

$$\mathrm{E} = \sum_{bonds} \mathrm{K}_r (r - r_0)^2 \tag{1.7}$$

$$\mathrm{E} = \sum_{angles} \mathrm{K}_\theta (\theta - \theta_0)^2 \tag{1.8}$$

The constraints are taken from another force field called AMBER all atom force field.

$$\mathrm{E} = \sum_{i} \frac{\mathrm{V}_1}{2}[1 + \cos(\phi + \phi_0)] + \frac{\mathrm{V}_2}{2}[1 - \cos 2(\phi - \phi_0)] + \frac{\mathrm{V}_3}{2}[1 + \cos 3(\phi - \phi_0)] \tag{1.9}$$

In this formula, V_1, V_2, V_3 are the coefficients in the Fourier series. Finally, the total energy is

$$E = E_{bonds} + E_{angles} + E_{dihedrals} + E_{nonbonded} \tag{1.10}$$

Another force field used in this research was AMBER all atom force field. It has the similar function to calculate the interaction between atoms.

$$E = \sum_{bonds} K_r(r-r_0)^2 + \sum_{angles} K_\theta(\theta-\theta_0)^2 + \sum_i \frac{V_1^i}{2}[1+\cos(\phi_i+f_i i)] + \sum_{i<j}[\frac{q_i q_j}{4\pi\epsilon_0 r_{ij}} + \frac{A_{ij}^{12}}{r_{ij}^{12}} - \frac{C_{ij}^6}{r_{ij}^6}] \tag{1.11}$$

The f_i are the phase angles. The assumption of this force field is that such a simple representation can reproduce most situation of the unstrained systems. The goal of this force field is to accurately model conformational energies and intermolecular interactions involving proteins, nucleic acids, and other molecules with related functional groups which are of interest in organic and biological chemistry.

1.4.3 Intermolecular interactions

The particle mesh ewald (PME) method was used to evaluate electrostatic interaction as it is a computationally efficient method for handling large periodic systems [24, 25]. The cut-off range for electrostatic force and Van de Waals force we choose was 1.20 nm, which is also commonly used for polymer simulations.

1.4.4 Partial atomic charges (PACs)

Partial atomic charges (PACs) of a molecule are important since values of the charges will affect the intra and intermolecular interactions (e.g. hydrogen bonds). There are different types of charge assignment methods. In this research, we focus on the four types of charge assignment methods.

1.4.4.1 COMPASS PACs

The first method was from the COMPASS force field. Bond-increments δ_{ij} were used, which signify the charge separation between two valence-bonded atoms i and j [26]. For an atom i, the partial atomic charge is the sum of charge bond increments δ_{ij}.

$$q_i = \sum_j \delta_{ij} \tag{1.12}$$

1.4.4.2 OPLS PACs

The second method was from the OPLS force field. The charges for the OPLS force fields are empirical and have been obtained from fitting to reproduce properties of certain system [27]. Testing properties of system leads to the adjustment of charge assignment or even the Lennard-Jones parameters.

1.4.4.3 Gasteiger PACs

The third method is the Gasteiger-Marsili empirical partial atomic charges [28]. Atomic charges are obtained by making use of the principle of electronegativity

equalization. The Gasteiger method is an electrostatic model which leads to only partial equalization of the orbital electronnegativity. In this way, the charges relate well with physical and chemical properties. The model uses the Mulliken defination of electronegativity $\chi = 0.5(IP + EA)$. The function joins three electronegativity values of an atom in its anionic, neutral, and cationic state by a parabola form. It uses the formation like

$$\chi = aQ^2 + bQ + c \tag{1.13}$$

By using the proper ionization potential and electron affinities, the constants a, b and c can be obtained. The final equation for a total charge Q_i on the atom i in the polyatomic molecule is

$$Q_i = \sum_{\alpha} \left\{ [\sum_{j} \frac{1}{D_j}(\chi_j - \chi_i) + \sum_{k} \frac{1}{D_k}(\chi_k - \chi_i)]((\frac{1}{f})^{\alpha-1}) \right\} \tag{1.14}$$

Here, j and k represent neighbours of i that are more or less electronegative than i, D_j and D_k are the electronegativity difference. The electronegativity difference does not affect the performance of this model seriously. Change in this part will cause only minor shift in the absolute values of the atom charges. α is the iteration steps. The iteration succeeds when the shift of value of the charge is less than 0.0002 electrons.

1.4.4.4 QEq PACs

The fourth method is called charge equilibration method (QEq)[29]. The charges of atoms are equilibrated by the charge dependence on the atomic energy and inter

atomic energy. The QEq approach uses the experimental ionization potential, electron affinity and atomic radius. Changes of the environment can be taken into consideration with this method. This method is suitable for assigning partial charges to the polymer materials. The QEq method proposes a charge adjustment due to the geometry and experimental atomic properties, which can be applied to large molecules. The calculation process is as followed [29, 30]. The QEq method starts the work by relating the charge with atomic energy. In order to estimate the equilibrium of charges in a molecule, the energy of isolated atom is a function of charge.

$$\mathrm{E}_A(\mathrm{Q}) = \mathrm{E}_{A0} + \mathrm{Q}_A(\frac{\partial \mathrm{E}}{\partial \mathrm{Q}})_{A0} + \frac{1}{2}\mathrm{Q}_A^2(\frac{\partial^2 \mathrm{E}}{\partial \mathrm{Q}^2})_{A0} + ... \tag{1.15}$$

In a general way, the terms till the second order are remained for further calculation.

$$\mathrm{E}_A(+1) = \mathrm{E}_{A0} + (\frac{\partial \mathrm{E}}{\partial \mathrm{Q}})_{A0} + \frac{1}{2}(\frac{\partial^2 \mathrm{E}}{\partial \mathrm{Q}^2})_{A0} \tag{1.16}$$

$$\mathrm{E}_A(-1) = \mathrm{E}_{A0} - (\frac{\partial \mathrm{E}}{\partial \mathrm{Q}})_{A0} + \frac{1}{2}(\frac{\partial^2 \mathrm{E}}{\partial \mathrm{Q}^2})_{A0} \tag{1.17}$$

$$\mathrm{E}_A(0) = \mathrm{E}_{A0} \tag{1.18}$$

$$(\frac{\partial \mathrm{E}}{\partial \mathrm{Q}})_{A0} = \frac{1}{2}(IP + EA) = \chi_A^0 \tag{1.19}$$

$$\frac{\partial^2 \mathrm{E}}{\partial \mathrm{Q}^2} = IP - EA = \mathcal{J}_A A^0 \tag{1.20}$$

In this two equations, the IP and EA mean the ionization potential and electron affinity. Then

$$\mathrm{E}(\mathrm{Q}) = \mathrm{E}_{A0} + \chi_A^0 \mathrm{Q}_A + \frac{1}{2}\mathcal{J}_A A^0 \mathrm{Q}_A^2 \tag{1.21}$$

In order to calculate the charge distribution for a large molecule, the inter atomic electrostatic energy should be included.

$$\mathrm{E}(\mathrm{Q}_1...\mathrm{Q}_N) = \sum_A (\mathrm{E}_{A0} + \chi_A^0 \mathrm{Q}_A + \frac{1}{2}\mathcal{J}_A A^0 \mathrm{Q}_A^2) + \sum_{A<B} Q_A Q_B \mathcal{J}_{AB} \tag{1.22}$$

Taking the derivative of E will lead to an atomic-scale chemical potential form.

$$\chi_A(Q_1...Q_N) = \frac{\partial \mathrm{E}}{\partial \mathrm{Q}} = \chi_A^0 + \sum_B \mathcal{J}_{AB} \mathrm{Q}_B \tag{1.23}$$

For equilibrium, the atomic chemical potentials should be equal.

$$\chi_1 = \chi_2 = ... = \chi_N \tag{1.24}$$

For the total charge of the system,

$$\mathrm{Q}_{total} = \sum_{i=1}^{N} \mathrm{Q}_i \tag{1.25}$$

We can notice that, in this way, the partial atomic charge for hydrogen is different from each other. In other method, the partial atomic charge for hydrogen is same for each other.

1.4.5 Water models

In this work, we used three different water models including SPC/E, TIP3P and TIP4P. In general, the TIP4P water model works well with the OPLS-AA force

field. Here, the TIP4P water model is a 4-site model introduced by Bernal-Fowler model [31]. The TIP4P model was first published in 1983 by Jorgensen [32]. In the model, charges are not only placed on the consitutent atoms of a water molecule but also on a dummy atom (negatively charged) located underneath the oxygen along the bisector of the HOH angle. Such a model improves the charge distribution around the water molecule.

The TIP3P water model is one of the three-site models [32]. It has three interaction sites located at the three atoms of the water molecule. Each atom is assigned a point charge. The 3-site models are very popular for molecular dynamics simulation because of their simplicity and computational efficiency. Such models use a rigid geometry matching the known geometry of the water molecule.

The SPC/E is one of the most commonly used 3-site models. It should be pointed out that the ideal tetrahedral shape angle 109.47° of HOH angle is used instead of 104.5°, which is observed from experiment.

The comparison of three water models is listed in the Table 1.1.

In the Table 1.1, σ signifies the radius of water molecule. The ϵ is the energy. The l_1 is the distance of the oxygen to the hydrogen. l_2 is the distance of the charge center of oxygen to the mass center of the oxygen. The q_1 is charge of the hydrogen atom and q_2 is the charge of the oxygen atom. The $\theta°$ is the angle of hydrogen to oxygen mass center to hydrogen. The $\varphi°$ is the angle of hydrogen to oxygen mass center to oxygen charge center. The physical properties of water calculated using the three water models are show in Table 1.2 [33–37].

TABLE 1.1: TIP4P, TIP3P, SPC/E water models and experimental values

	TIP4P	TIP3P	SPC/E	Experimental value
$\sigma \mathring{A}$	3.15365	3.15061	3.166	2.750
$\epsilon\ kjmol^{-1}$	0.6480	0.6364	0.650	-
$l_1 \mathring{A}$	0.9572	0.9572	1.0000	0.9572
$l_2 \mathring{A}$	0.15	-	-	-
$q_1(e)$	+0.5200	+0.4170	+0.4238	-
$q_2(e)$	-1.0400	-0.8340	-0.8200	-
θ°	104.52	104.52	109.47	104.47
φ°	52.26	-	-	-

TABLE 1.2: Physical properties of water caculated using TIP4P, TIP3P and SPC/E water models along with experimental values

	TIP4P	TIP3P	SPC/E	Experimental value
Dipole moment	2.18	2.35	2.35	-
Dielectric constant	53	82	71	80 (20°C)
self-diffusion,$10^{-5} cm^2/s$	3.29	5.19	2.49	2.299 (25°C)
Configurational energy, kJ mol^{-1}	-41.8	-41.1	-41.5	-
Density maximum, $^\circ C$	-25	-91	-38	4
Expansion coefficient, $10^{-4} \circ C^{-1}$	4.4	9.2	5.14	9.0 (20°C)

1.4.6 Thermostat

Thermostats are designed to control the temperature of system at a set value along with proper fluctuations around it. There are several temperature coupling methods available in the GROMACS simulation package. The Berendsen temperature coupling and Nose-Hoover temperature coupling are the two most common methods [38]. The Berendsen coupling method controls the system temperature with an external heat bath with a set temperature. The temperature will become stable and fluctuate in a small range if Berendsen thermostat is chosen with a small

relaxation time constant. It is an accurate and reliable method to stabilize the system's temperature. The Nose-Hoover thermostat method is another important temperature coupling method. Compared to the Berendsen thermostat, the Nose-Hoover method is able to obtain proper canonical ensemble fluctuations. On the other hand, the Berendsen thermostat does not provide a correct kinetic energy distribution of the system. In this work, we used both thermostats. The research aims at getting the dynamic properties of the PolyNAGA system. The method is to use Berendsen thermostat to couple the temperature to the set temperature quickly and then use Nose-Hoover to run simulation to collect data.

1.4.7 Barostat

In the NPT ensemble, in addition to the temperature, one needs to control the pressure. In general, the pressure coupling algorithms adjust the size of the simulation unit cell and scale the coordinates of the atoms. Compared to the thermostat, barostats tend to generate larger fluctuations. The two types of pressure coupling methods are Berendsen and Parrinello-Rahman. The Berendsen barostat metohd does not provide the real dynamic ensemble. So in this research, the Parronello-Rhman barostat was used.

Chapter 2

Effect of partial atomic charges on the conformation of a short, single polyNAGA chain in water

To study the effect of partial atomic charges on the conformation of polyNAGA in water at different temperatures, we used a single, short (10 monomers) and atactic polyNAGA chain along with different force fields, methods for the estimation of partial atomic charges and water models. Initial structures of polyNAGA, which were subjected to three-dimensional periodic boundary conditions, were built using commercial software Materials Studio. The initial structures were then exported to GROMACS for subsequent MD simulations. The simulations were carried out using the Westgrid computing network.

To equilibrate the sturctures, the isobaric-isothermal (NPT) ensemble was used

for the simulations. The pressure of periodic unit cell was controlled at 1.0 bar by the Parrinello-Rahman barostat. The time constant for coupling was 1.0 ps. The thermostat used for controlling temperature was Nose-Hoover method. Temperatures near the experimentally observed UCST of polyNAGA were used. The Nose-Hoover thermostat coupling time was 0.2 ps. The coupling time used was adequate to control the temperature within 3 K of the targeted temperatures. The Particle Mesh Edwald (PME) method with a cutoff distance of 1.2 nm was used to handle the long-range electrostatic interactions. The Fourier spacing used was 0.12. The cutoff distance for the van der Waals interaction was also set to 1.2 nm. The grid neighbor searching method was used to speed up the van der Waals energy calculation. The leap-forg Verlet method was used to integrate the equations of motion of all atoms and the time step used was 1 fs.

2.1 Model construction of polyNAGA10

As mentioned, commercial software Materials Studio was used to generate the initial models. In particular, the Amorphous Cell module was used to build a single polyNAGA chain in a cubic unit cell subjected to three-dimensional periodic boundary conditions. The resulting unit cell had an edge length of 4 nm. The density of system is 0.034 g/cm^3. It was far lower than the bulk density of polyNAGA. But cell would be filled with water later. Energy minimization along with the steep force field was carried out to eliminate the bad contacts between atoms. After the energy minimization, the structure was then exported in the protein data bank (pdb) file format (see Appendix A) to GROMACS.

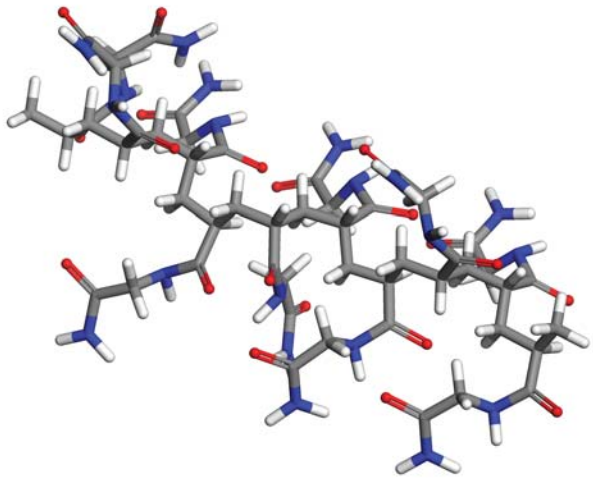

FIGURE 2.1: The structure of polyNAGA10

For the 10 repeat units system of polyNAGA (polyNAGA10), the structure was built with the form of atactic homopolymer. In this way, the side chains of the polymer were assigned randomly and alternately on the backbone (see figure 2.1). After the model established on the atomistic document, the position information was acquired. In the Materials Studio package, the Amorphous Cell package was used to built the polymer chains in the bulk state. After the energy minimization, the document was outputted as atomic position file for the GROMACS simulation. The file format is the Protein Data Bank format (PDB) (See Appendix A).

The pdb file was latter complied into the topology file which was used for the subsequent MD simulation (see Appendix B). At this point, water molecules were added into the cubic unit cell to surround the polyNAGA molecule. The number of water molecules added was 2,109. This corresponds to a concentration of polyNAGA in water to about 3.3 wt%. The edge length of the cubic unit cell was 4 nm. For this preliminary study, we used low concentration of polyNAGA. The entire solution system was energy minimized using the parameter specified in the Appendix C.

MD simulation was then performed using a mdp file on the resulting system (see Appendix D). In the ".mdp" file, the time of simulation, the time step, the temperature value and its control method, and the pressure value and its control method are specified.

In order to measure the conformation of polyNAGA, the radius of gyration was calculated. The radius of gyration at a given time is defined as:

$$R_g = (\frac{\Sigma_i ||r_i|| m_i}{\Sigma_i m_i})^{\frac{1}{2}} \tag{2.1}$$

r_i is the norm of vector from site i to the gravity center of the polymer chain. And m_i is the mass the site i. Therefore, one can use the R_g of a polymer in the solution to infer its solubility qualitatively.

The number of hydrogen bonds is another measured quantity. Hydrogen bond is defined geometrically :(1) the cutoff radius between acceptor and donor is 0.35 nm. (2) the cut off angle of hygrogen - donor - acceptor is less than 30 degree.

2.2 PolyNAGA10 with COMPASS charges

The partial atomic charges of a polymer are important as they influence the non-bonded interaction. There are many types of partial atomic charge assignment methods. As mentioned, we used four different types of charge assignment methods, COMPASS, OPLS-AA, Gasteiger and QEq.

TABLE 2.1: Partial atomic charges of a polyNAGA monomer assigned by various methods

Atom	COMPASS	OPLS-AA	Gasteiger	QEq
C1	-0.106	-0.120	-0.031	-0.268
H11	0.053	0.060	0.028	0.197
H12	0.053	0.060	0.028	0.173
C2	-0.053	-0.060	0.031	-0.102
H21	0.053	0.060	0.039	0.190
C3	0.450	0.500	0.203	0.444
O1	-0.450	-0.500	-0.277	-0.531
N1	-0.574	-0.500	-0.249	-0.514
H1	0.351	0.300	0.132	0.316
C4	0.117	0.080	0.082	-0.085
H41	0.053	0.060	0.054	0.138
H42	0.053	0.060	0.054	0.195
C5	0.450	0.500	0.231	0.440
O2	-0.450	-0.500	-0.274	-0.574
N2	-0.702	-0.760	-0.369	-0.567
H2	0.351	0.380	0.159	0.289
H3	0.351	0.380	0.159	0.259

Table 2.1 shows the four types of partial atomic charges of the monomer unit using COMPASS, OPLS-AA, Gasteiger and QEq method. From Table 2.1, compared

to other methods, the Gasteiger method assigned lower absolute value charges to the H-acceptor O and H-donor N. COMPASS charges and OPLS-AA charges are similar since both of them are assigned based on the bond increments theory. QEq charges have the largest absolute values than any other types of charges.

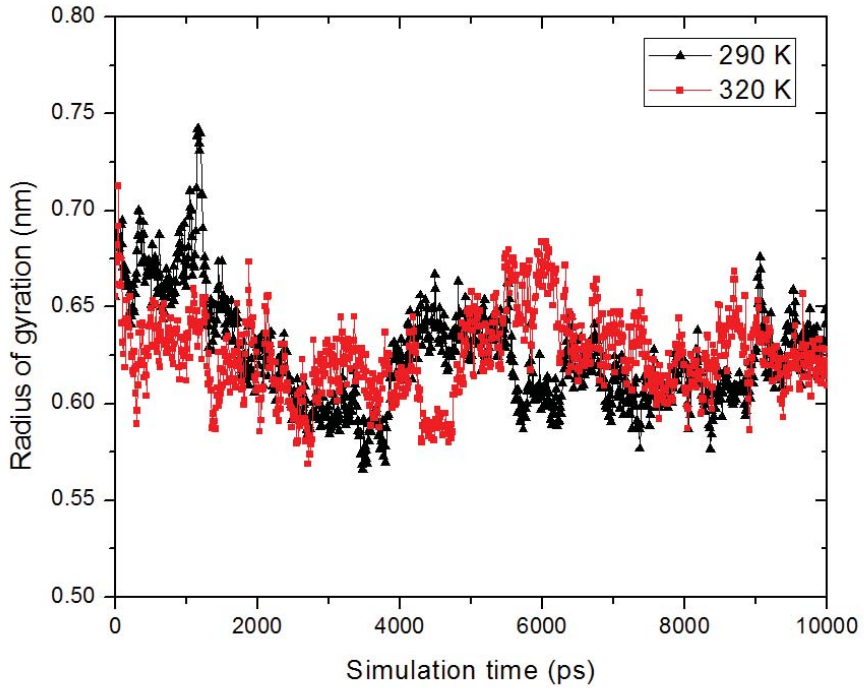

FIGURE 2.2: Radii of gyration of polyNAGA10 with COMPASS charges as a function of time at 290 K and 320 K

Figure 2.2 shows radii of gyration of polyNAGA10 with COMPASS charges. The comparison is done between two different temperatures, 290 K and 320 K. we performed 10 ns simulation for this system because the polymer chain was short. The radius of gyration fluctuated around 0.62 nm and did not very much. From Figure 2.2, the radius of gyration at 290 K is almost the same as that at 320

K. In other words, the COMPASS charges were not able to capture the expected temperature dependence of the radius of gyration of polyNAGA.

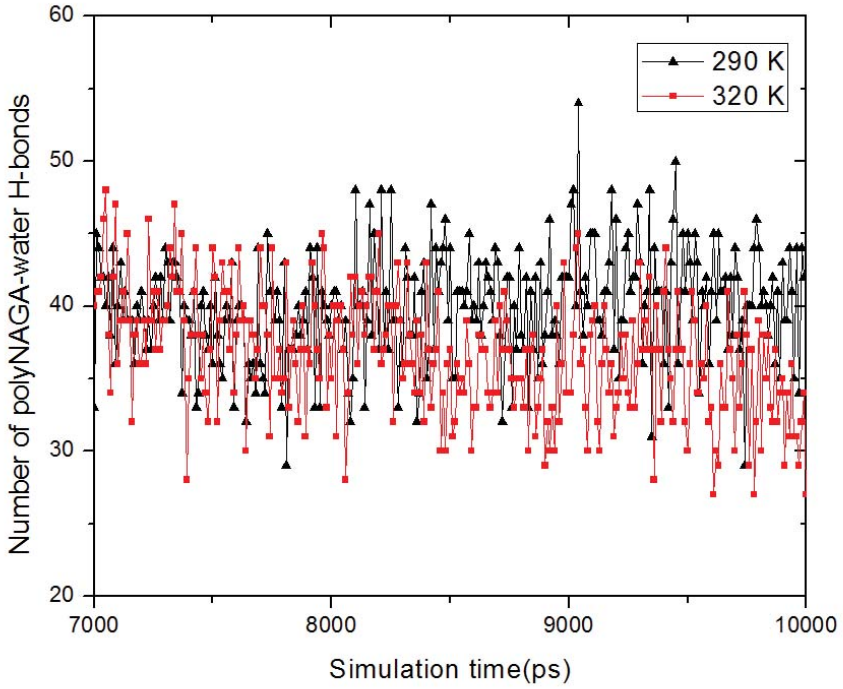

FIGURE 2.3: Numbers of polyNAGA10-water H-bonds at 290 K and 320 K

Numbers of two types of hydrogen bonds were investigated. Figure 2.3 shows numbers of polymer with water hydrogen bonds by using the last 3 ns of simulation. Numbers of hydrogen bonds at 290 K and 320 K did not differ significantly. When the average numbers were calculated, numbers of hydrogen bonds of polymer with water at 290 K were 40 $\pm$ 7 and at 320 K were 36 $\pm$ 6. This suggested that polyNAGA formed more hydrogen bonds at a lower temperature. Numbers of hydrogen bonds within polyNAGA at 290 K and 320 K are shown in the Figure 2.4. From the figure, numbers of hydrogen bonds within side chains at 290 K and that at 320 K were more or less the same.

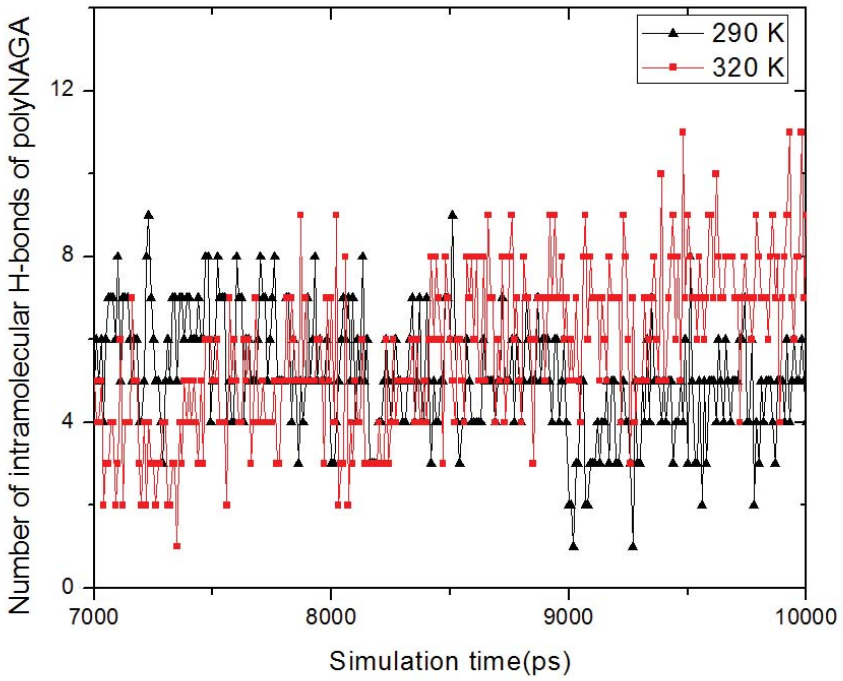

FIGURE 2.4: Numbers of intramolecular polyNAGA10 H-bonds at 290 K and 320 K

2.3 PolyNAGA10 with OPLS-AA charges

In this section, we reported the results of polyNAGA10 with OPLS-AA charges. The computed radii of gyration at 290 K and 320 K were comparable. In order to get a more obvious result, the comparison of temperatures was set to 280 K and 360 K. Figure 2.5 shows radii of gyration of polyNAGA10 with OPLS charges at 280 K and 360 K. From this figure, we could see, for this type of charge assignment method, the radius of gyration at 280 K and 360 K did not have a big difference. For the 360 K, the fluctuation was bigger than at 280 K. But the average level of gyration radius over time bore no difference. For this case, the data selection was from 7000 ps (7 ns) since the system was stable after 7 ns.

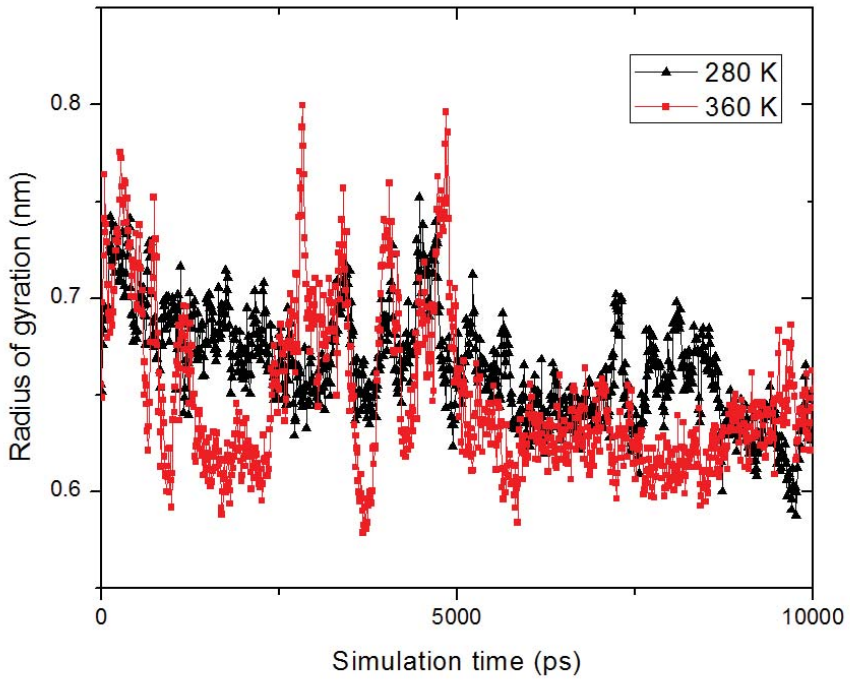

FIGURE 2.5: Radii of gyration of polyNAGA10 with OPLS charges at 280 K and 360 K

Figure 2.6 shows H-bonds of polyNAGA-water. When the average number was calculated, numbers of hydrogen bonds of polymer with water at 280 K were 50 ± 7 and at 360 K were 40 ± 8. This suggested that, same with COMPASS charges, polyNAGA built with OPLS charges formed more hydrogen bonds at a lower temperature.

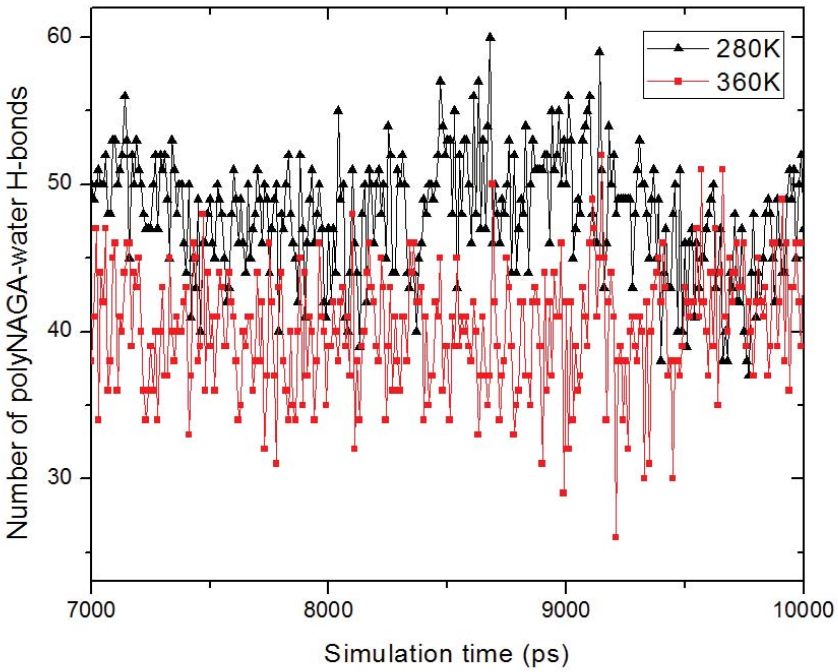

FIGURE 2.6: Numbers of H-bonds of polyNAGA10 with water with OPLS charges at 280 K and 360 K

Figure 2.7 shows the H-bonds within polyNAGA chain. Numbers of intra H- bonds of polyNAGA at 280 K were 3 ± 1 and at 360 K were 4 ± 1. At 360 K, numbers of intra H-bonds was slightly larger than that at 280 K.

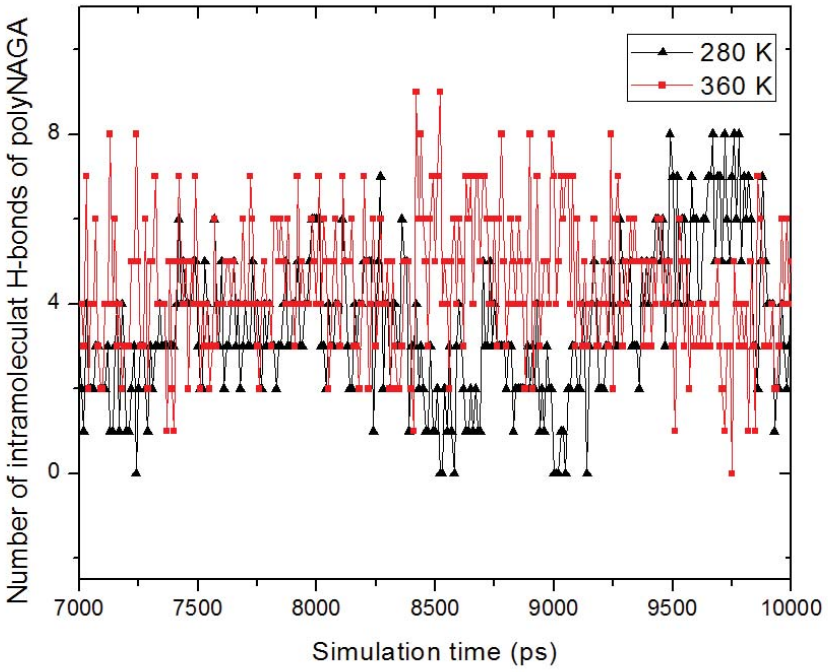

FIGURE 2.7: Numbers of H-bonds of polyNAGA10 within chain with OPLS charges at 280 K and 360 K

2.4 PolyNAGA10 with QEq charges

In this section, the QEq method was used to assign partial atomic charges to polyNAGA.

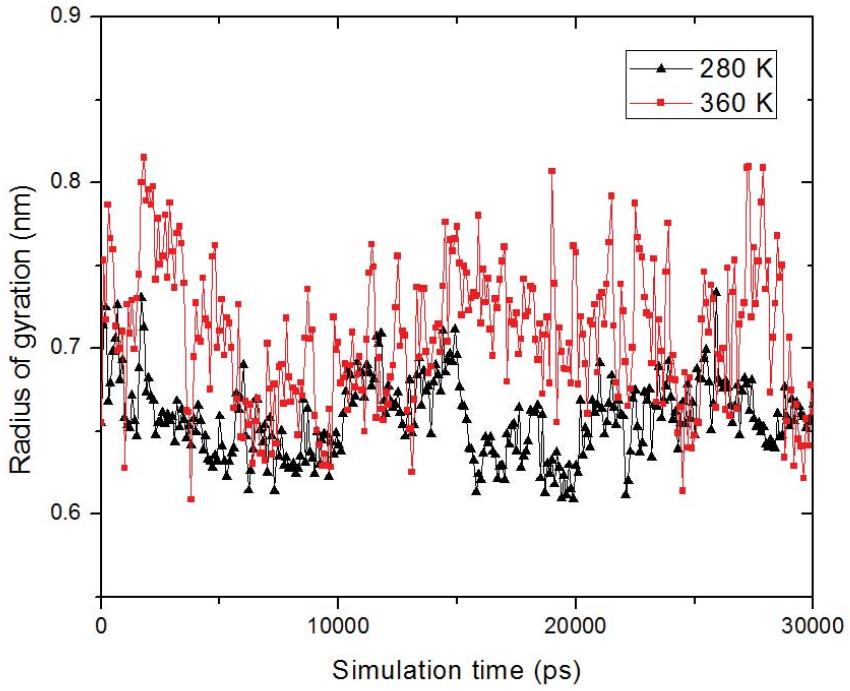

FIGURE 2.8: Radii of gyration of polyNAGA10 with QEq charges at 280 K and 360 K

After the partial atomic charges assignment, MD simulations were carried out for 30 ns at different temperatures. The radii of gyration at 280 K and 360 K were recorded and compared. Figure 2.8 shows radii of gyration of polyNAGA10 with QEq charges at 280 K and 360 K. From the figure, we could see for this type of charge assignment method, the radius of gyration at 360 K was slightly larger than that at 280 K. The average radius of gyration at 280 K was 0.66 $\pm$ 0.04 nm and at 360 K was 0.71 $\pm$ 0.06 nm. In this result, it seemed that the QEq charge

assignment method was able to capture the temperature dependence of radius of gyration.

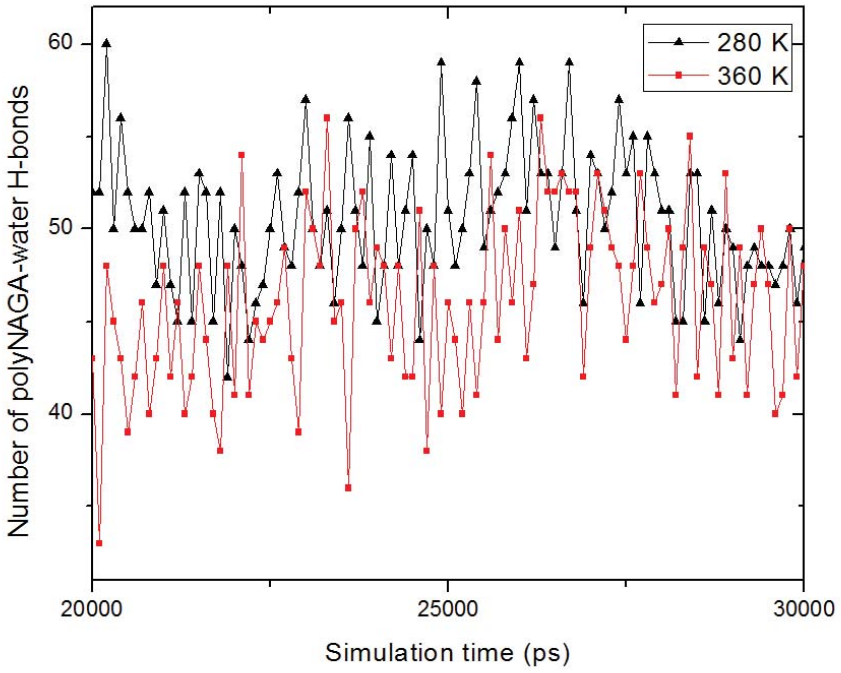

FIGURE 2.9: Numbers of polyNAGA10-water H-bonds at 280 K and 360 K

Figure 2.9 shows numbers of polyNAGA-water H-bonds. Numbers of hydrogen bonds of polymer with water at 280 K were 50 ± 4 and at 360 K were 46 ± 5. Numbers of H-bonds of polymer with water at 360 K was slightly smaller than that at 280 K.

Figure 2.10 calculated numbers of intramolecular H-bonds of polyNAGA10. Numbers of H-bonds of polymer within chain at 280 K were 3 ± 1 and at 360 K were 3 ± 2. Numbers of H-bonds within polyNAGA chain were more or less the same at 360 K and 280 K.

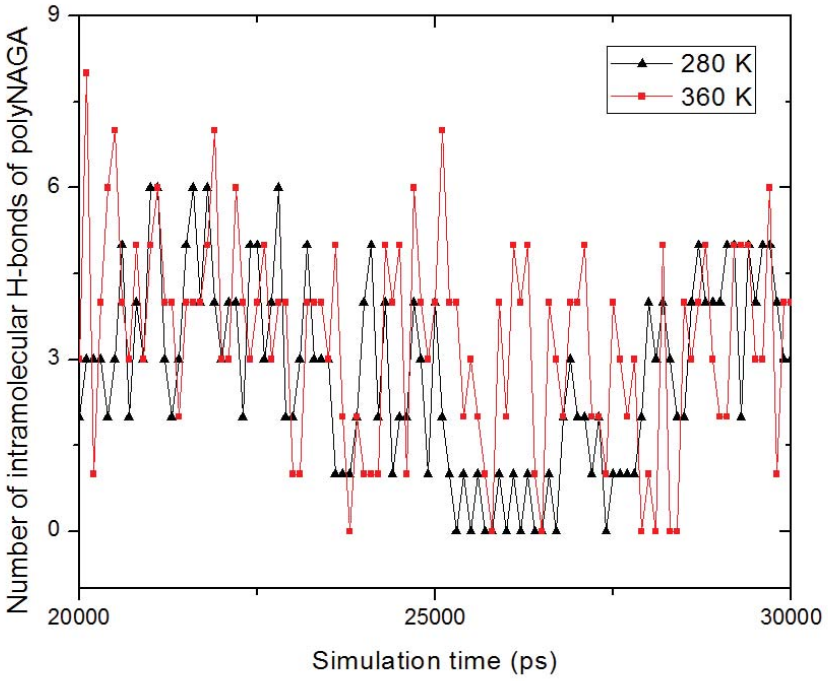

FIGURE 2.10: Numbers of intramolecular H-bonds of polyNAGA10 at 280 K and 360 K

2.5 PolyNAGA10 with Gasteiger charges

In this section, the Gasteiger method was used to assign partial atomic charges to polyNAGAq10 [28].

After the charge assignment, NPT MD simulations were carried out 30 ns at different temperatures. Radii of gyration of polyNAGA at 280 K and 360 K were calculated. Figure 2.11, the average number of radius of gyration for 280K was 0.56 ± 0.01 nm and for 360K was 0.65 ± 0.04 nm.

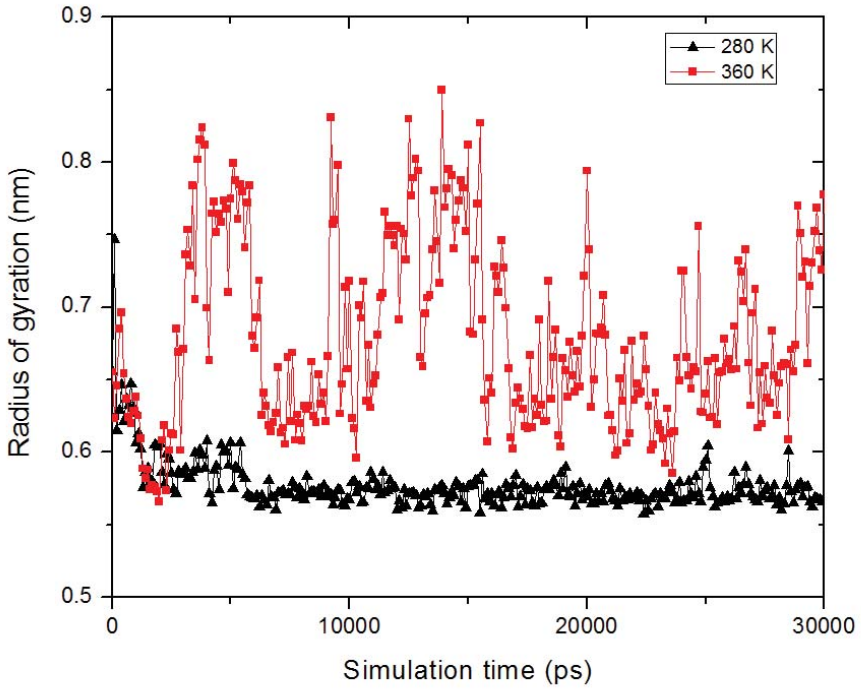

FIGURE 2.11: Radii of gyration of polyNAGA10 with Gasteiger charges at 280 K and 360 K

The Gasteiger assignment method yielded a clear UCST trend. After that, four different temperatures, 280 K, 300 K, 320 K and 360 K were used for further MD

simulation. Figure 2.12, radii of gyration at four temperatures were listed. The radius of gyration increased from 0.56 nm ± 0.01 at 280 K to 0.65 nm ± 0.04 gradually. Experimentally, The cloud point temperature of 1.0 wt% poly(NAGA) in pure water is 22-23 °C [1]. In this case, the cloud point of 3.3 wt% polyNAGA solution is near 23 °C. It was found that numbers of the poly(NAGA)-water hydrogen bonds were insensitive to temperature (see Figure 2.14). However, the intra-molecular hydrogen bonds of poly(NAGA) decreased slightly with increasing temperature (see Figure 2.13). The decreasing trend may explain why did

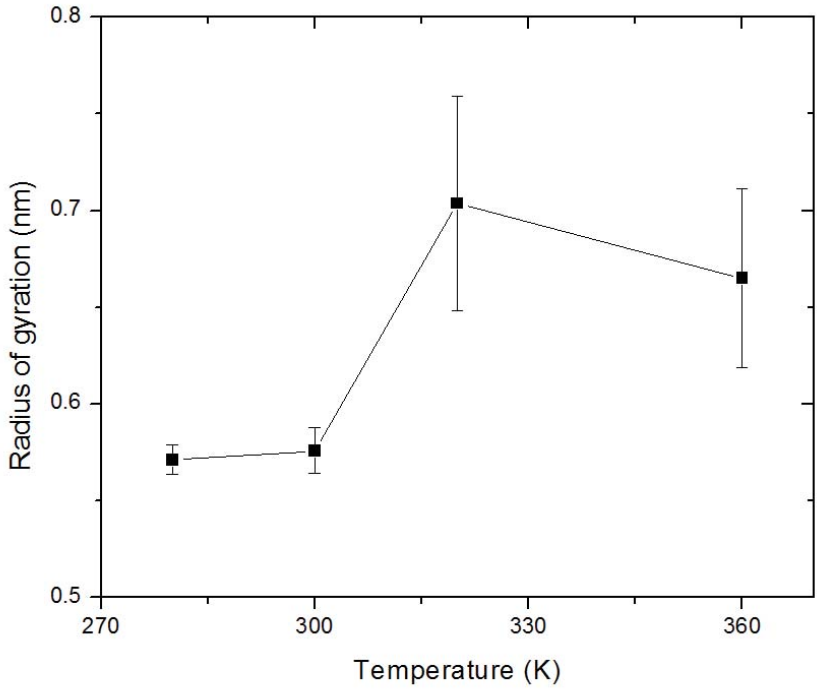

FIGURE 2.12: Radii of gyration of polyNAGA10 with Gasteiger charges at 280 K, 300 K, 320 K and 360 K

polyNAGA10 adopt a more expanded conformation at high temperatures. This is related to the lower absolute value of the charges of the hydrogen bonds moieties compared to other charge assignment methods.

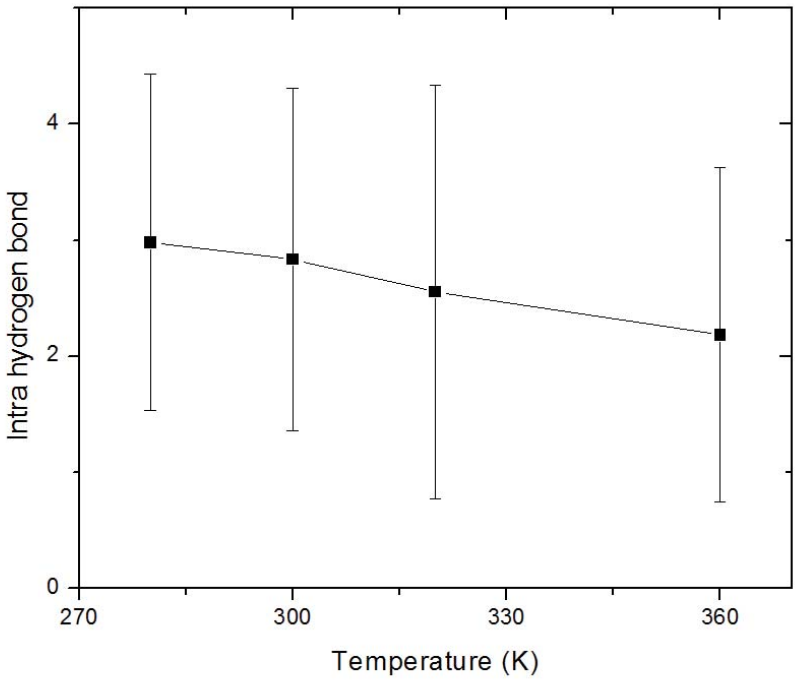

FIGURE 2.13: Numbers of intramolecular polyNAGA10 H-bonds over temperature range of 280 - 360 K

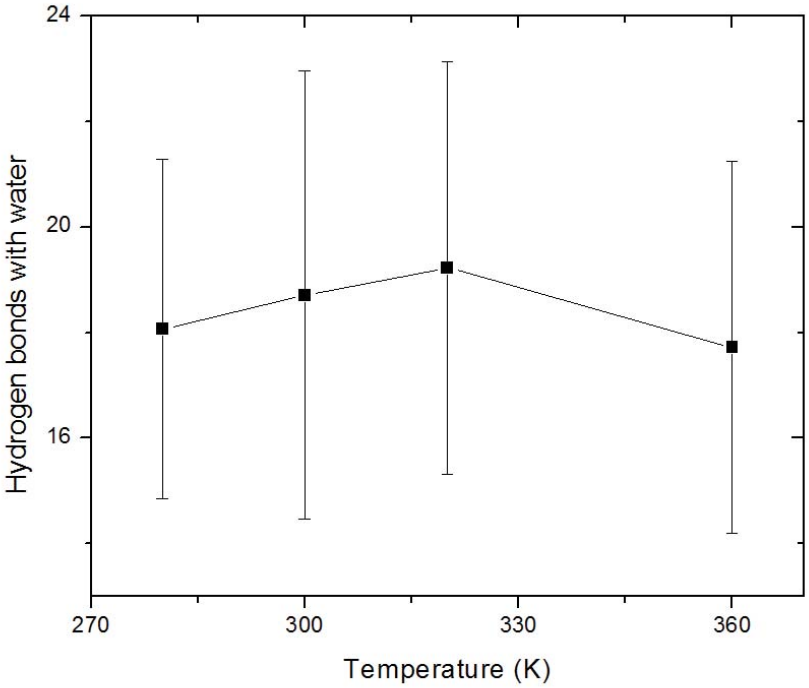

FIGURE 2.14: Numbers of polyNAGA10-water H-bonds over temperature range of 280 - 360 K

2.6 Conclusion

Considering the computational cost, we first used a polyNAGA model with only 10 repeating units. It is worth pointing out that the longer the chain one uses, the more water molecules are needed to achieve the required concentrations. In this chapter, different types of charge assignment methods were used to test which would reproduce the upper critical solution temperature behaviour of polyNAGA. The force field and the water model used in this chapter were OPLS-AA force field and TIP4P.

Four types of charge assignment methods were used including the COMPASS charges, the OPLS-AA charges, the QEq charges and the Gasteiger charges. The comparison of different charge assignments was discussed. The suitable charge assignment method would not lead to the collapse of polymer chain upon heating. It was found that the COMPASS and OPLS-AA charges were not able to reproduce the UCST phenomenon. The QEq method was able to show the trend but it is not obvious. The Gasteiger charges can be used to reproduce the UCST behavior of polyNAGA. The UCST behavior was attributed to the decrease in intra-molecular hydrogen bonds upon increasing temperature.

Chapter 3

Conformation of a single polyNAGA30 chain in water

In this Chapter, we reported the results on the conformation of a single, atactic polyNAGA chain with 30 repeating units in water. The molecular weight of the polyNAGA chain with 30 repeating units was 3,856 g/mol which is comparable to that of polyNAGA synthesized experimentally. The purpose of this work was to check if a polyNAGA chain with molecular weight comparable to that of the experimental material would exhibit similar phase behavior of polyNAGA reported in the last chapter. We used GROMACS version 4.6.2 to do the isobaric-isothermal molecular dynamics simulations. Similar to what we did in the last chapter, we used different force fields, charge assignments method and different water models to study their effect on the conformation. We did not present the hydrogen bonds data in this chapter since the radius of gyration results suggested that no

combination of partial atomic charges, force fields and water models were able to reproduce the UCST trend.

3.1 Model construction of polyNAGA30

We basically followed the approach that we used to construct the polyNAGA solution in the last chapter. An initial cubic unit cell was constructed based upon the molecular weight of polyNAGA with 30 repeating units and its density. Energy minimization was performed. Water molecules were then added to the cubic unit cell to create the polyNAGA solution. The final dimensions of the unit cell was 6 nm, 6 nm and 6 nm and it contained 6,982. The corresponding concentration of polyNAGA in water was about 2.90 wt%. We used a simulation time of 50 ns for all MD simulations. The following sections summarized the corresponding results. However, it should be pointed out that the results of the long polyNAGA chain were different from those of the short chain. In this chapter, the OPLS-AA charges were not used since we found OPLS-AA charges are quite similar to COMPASS charges.

3.2 PolyNAGA30 with COMPASS charges

In this section, the COMPASS charges were assigned to polyNAGA. Meanwhile, two different types of force fields and three water models were used. Different

combinations of the force fields and water models were used to check which one(s) would yield the UCST behavior.

3.2.1 OPLS-AA force field and TIP4P water model

The OPLS-AA force field was used along with the COMPASS charges. The TIP4P water model was used. Figure 3.1 shows radii of gyration at 280 K and 320 K.

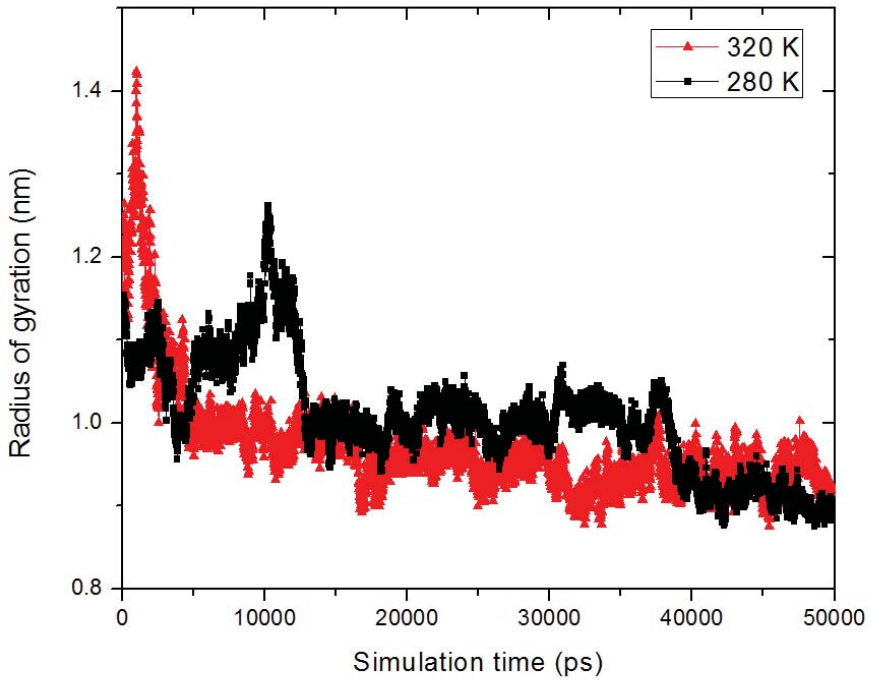

FIGURE 3.1: Radii of gyration at 280 K and 320 K, polyNAGA30 with COMPASS charges along with OPLS-AA force field and TIP4P water model

The data of radius of gyration was collected from 30 ns to 50 ns. From 30 ns, the system was stable enough. At 280 K, the radius of gyration was 0.96 ± 0.05 nm. At 360K, the radius of gyration was 0.93 ± 0.02 nm.

3.2.2 OPLS-AA force field and SPC/E water model

In this section, another water model SPC/E was used. The comparison of the TIP4P and SPC/E water model were listed in the chapter 1 [39].

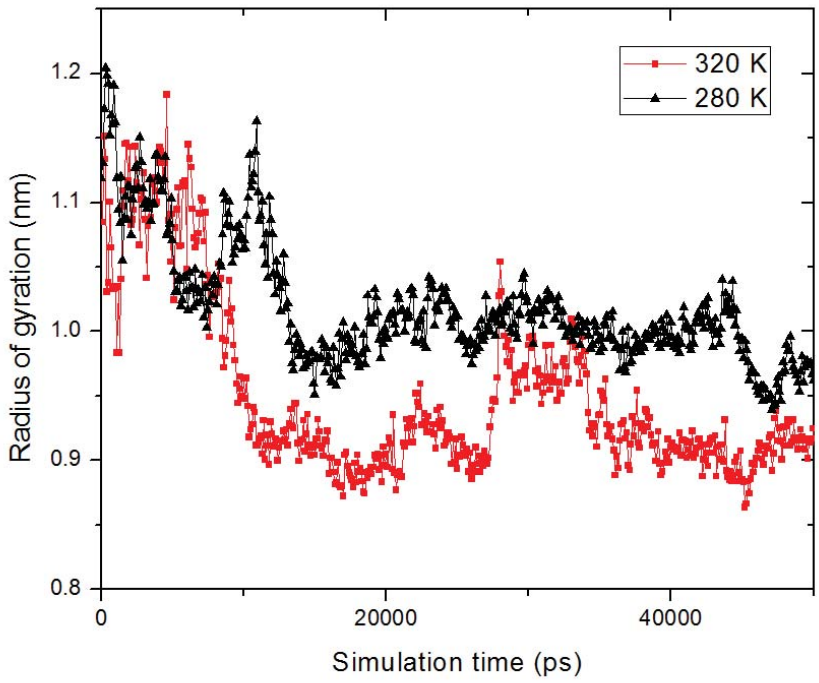

FIGURE 3.2: Radii of gyration at 280 K and 320 K, polyNAGA30 with COMPASS charges along with OPLS-AA force field and SPC/E water model

Figure 3.2 shows radii of gyration at 280 K and 320 K. The radius of gyration at 280 K was 0.99 ± 0.02 nm but at 320 K was about 0.92 ± 0.03 nm. The data from 30 ns to 50 ns was collected and calculated. It indicated an opposite behavior of UCST. When at low temperature, the polymer structure was more stretched. So in this way, the COMPASS charge assignment combing with SPC/E and OPLS-AA force field did not reproduce the UCST. When results of Figure 3.1 and Figure 3.2 were compared, it showed that the water model plays important

role in the formation of polymer chain conformation. Different water models have different possibilities to form hydrogen bonds which will influence the conformation of polymer.

The reason to choose TIP4P and SPC/E was based on the LCST research [40]. The TIP4P is a mature model for OPLS-AA force field. In general, simple models can be used in large systems and long simulations. And complex models and more accurate models can be used for small systems and short simulation times. For the TIP4P model, its well performance in reproducing the physical properties gives us good reason to use. The combination of TIP4P and OPLS-AA force field is the recommendation. For the water phase diagram reproducing, the TIP4P has the best performance. The SPC/E water model is more theoretic than TIP4P model. It uses angel of 109.47°, while TIP4P uses 104.52°. The 109.47° is the ideal tetrahedral shape (HOH angle of 109.47°). But for most of water models like TIP4P, the angle matches the real geometry of the water molecule.

3.2.3 AMBER force field and TIP3P water model

In this section, the AMBER force field was used. In the literature, the TIP3P water model is recommended for the AMBER force field. Compared with OPLS-AA force field, the AMBER parameter is more easier for representing the atom in the polymer chains. For the carbon atom, the general definition is CT. For the hydrogen, HC is usually used. But when the peptide bond needs to be built, hydrogen at the carbon which is the nearest to the nitrogen is usually named

H1. Though it has slightly difference with HC, the parameters of Lennard-Jonnes function are almost the same.

As noticed, parameters for the AMBER force field for different types of carbon and hydrogen are the same. In the Figure 3.3, the radius of gyration of polyNAGA30 with COMPASS charges along with AMBER force field and TIP3P water model was recorded at 280 K and 360 K. At 320 K, the radius of gyration was 1.03 ± 0.1 nm. At 280 K, the radius of gyration was 1.09 ± 0.02 nm.

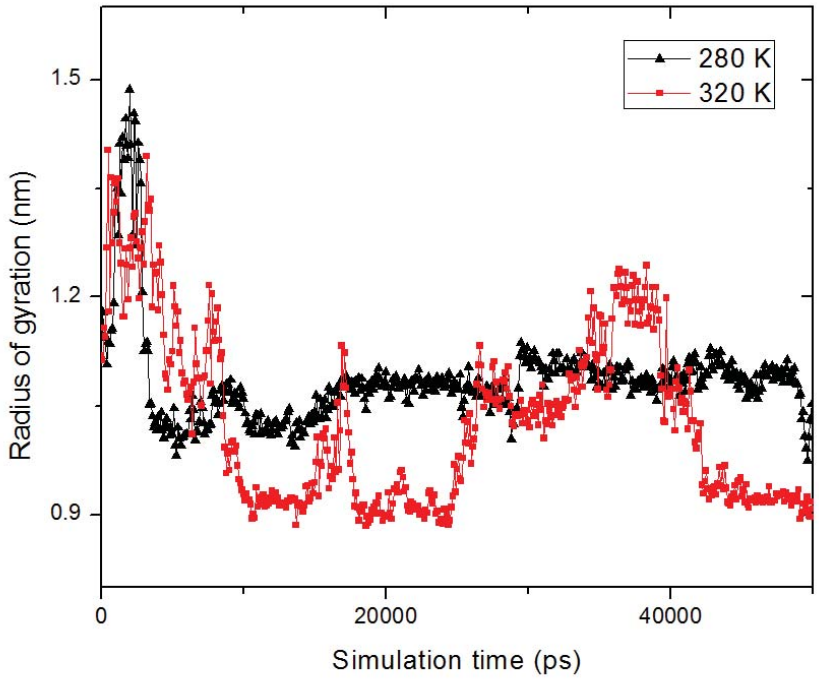

FIGURE 3.3: Radii of gyration at 280 K and 360 K, polyNAGA30 with COMPASS charges along with AMBER force field and TIP3P water model

3.3 PolyNAGA30 with QEq charges along with OPLS-AA force field and TIP4P water model

In this section, the QEq charges were used. Different from other sections, only combination of OPLS-AA force field and TIP4P water model was investigated. Radii of gyration at 280 K and 360 K were recorded. Figure 3.4, the radius of gyration of 360 K was fluctuating up to 1.70 nm. But at the final stage, it was stable around 1.0 nm. For the 280 K, the average level of radius of gyration was about 1.0 nm. For this type of charge assignment, the radius of gyration was increasing to 1.70 nm. That was a good sign for breaking the coiled up structure of polyNAGA in the previous. But in general, the average level of radius of gyration at 280 K and 360 K were the same. The data from 30 ns to 50 ns was used to calculate the average number of radius of gyration. At 280 K, the radius of gyration was 1.04 $\pm$ 0.05 nm. At 360 K, the radius of gyration was 1.04 $\pm$ 0.10 nm.

3.4 PolyNAGA30 with Gasteiger charges

From chapter 2, the Gasteiger charge was the most possible charge equilibrium method to get the UCST behavior since it was successful in the 10 repeat units system. So, different water models and force field parameters were combined to try to get a positive result of UCST phenomena.

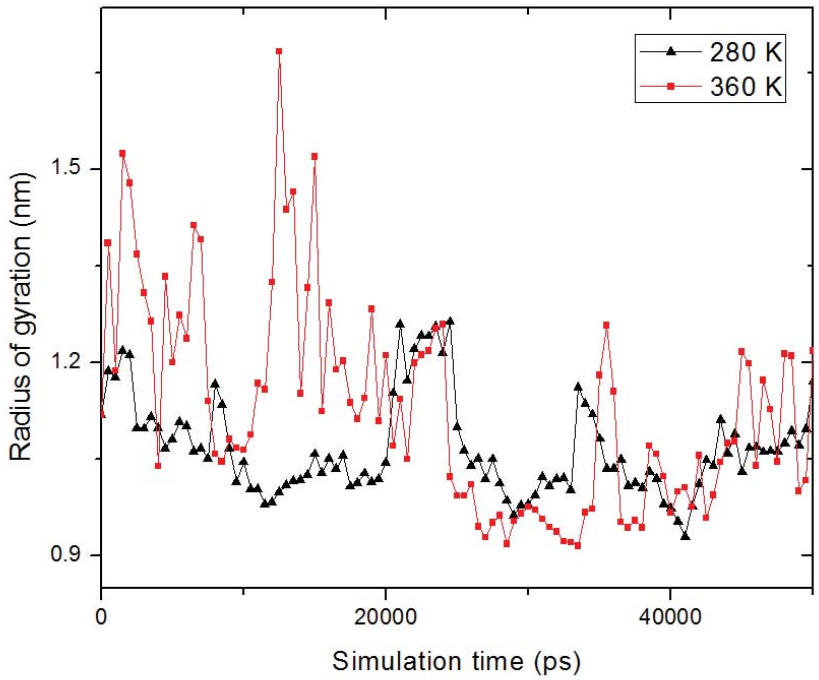

FIGURE 3.4: Radii of gyration at 280 K and 360 K, polyNAGA30 with QEq charges along with OPLS-AA force field and TIP4P

3.4.1 OPLS-AA force field and TIP4P water model

The Gasteiger charges assignment were used along with the OPLS-AA force field and TIP4P water model. Figure 3.5 shows the results on the computed radii of gyration at 280 K and 360 K.

In order to track the change of radius of gyration at different temperatures, more temperature points were selected. In Figure 3.6, computed radii of gyration at nine temperatures were shown. The results suggested that the radius of gyration of polyNAGA30 was insensitive to temperature.

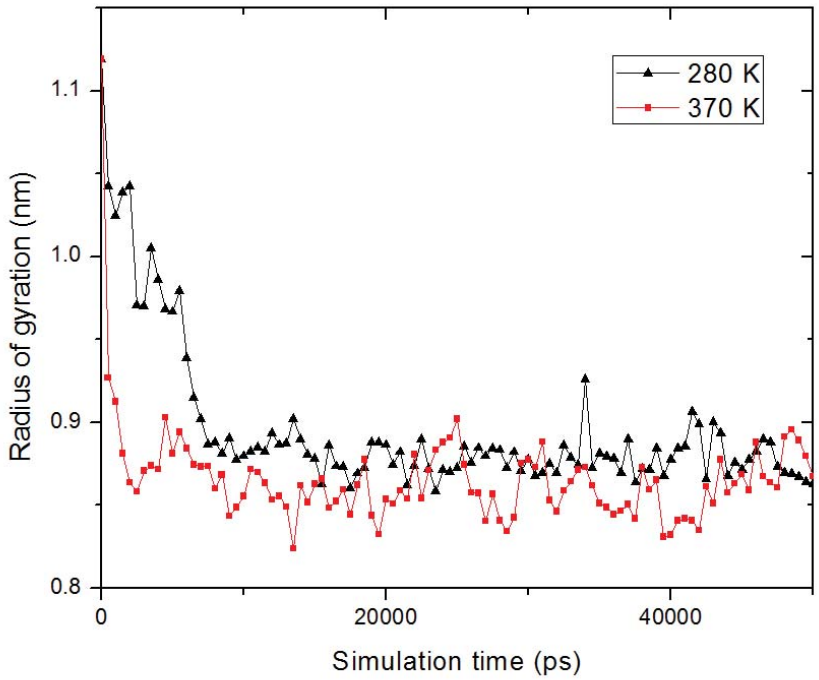

FIGURE 3.5: Radii of gyration at 280 K and 370 K, polyNAGA30 with Gasteiger charges along with OPLS-AA force field and TIP4P water model

Compared to the results of polyNAGA10, the Gasteiger charges seemed not to reproduce the UCST trend. The reason is unclear.

3.4.2 OPLS-AA force field and SPC/E water model

In this section, polyNAGA30 with Gasteiger charges along with OPLS-AA force field and SPC/E water model were used.

With the SPC/E water model, radii of gyration at 280 K and 360 K were not much different (see Figure 3.7). At 280 K, the radius of gyration was 0.87 ± 0.02 nm. At 360 K, the radius of gyration was 0.88 ± 0.02 nm.

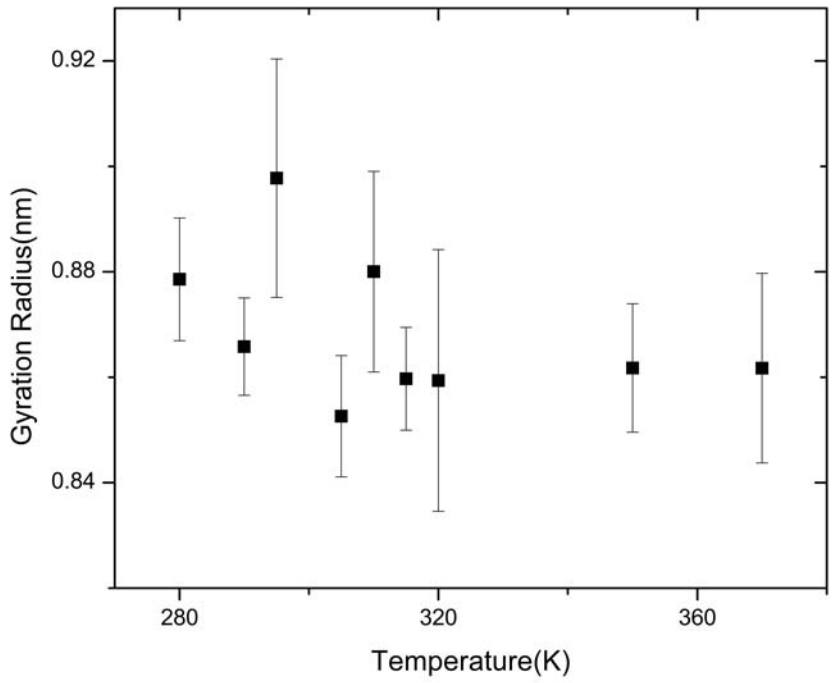

FIGURE 3.6: Radii of gyration at 280 K, 290 K, 295 K, 305 K, 310 K, 320 K, 350 K and 370 K, polyNAGA30 with Gasteiger charges along with and OPLS-AA force field and TIP4P water model

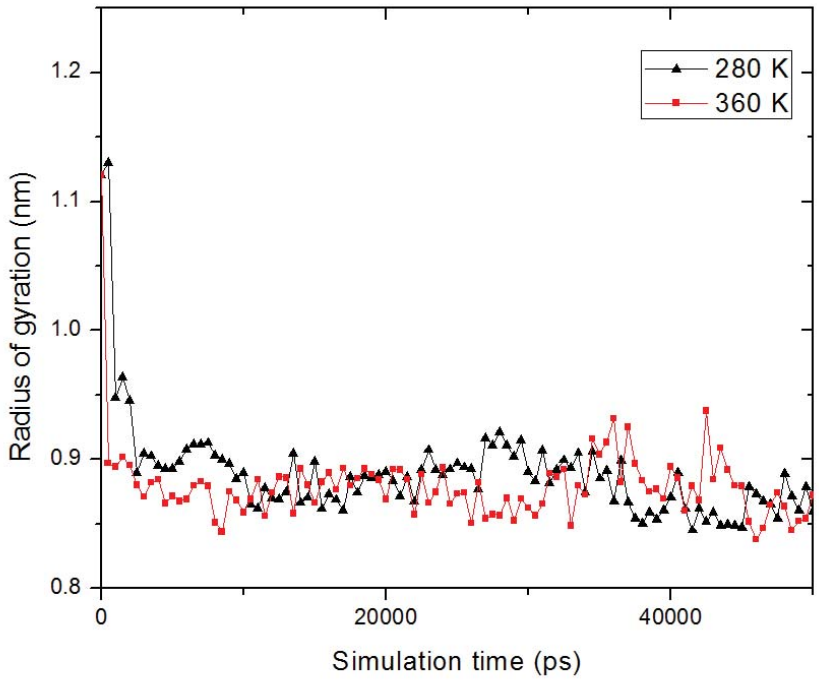

FIGURE 3.7: Radii of gyration at 280 K and 360 K, polyNAGA30 with Gasteiger charges along with OPLS-AA force field and SPC/E water model

3.4.3 AMBER force field and TIP3P water model

In this section, polyNAGA30 with Gasteiger charges along with AMBER force field and TIP3P were used for the MD simulation. Figure 3.8 shows radii of gyration at 280 K and 360 K. The radius of gyration decreased with increasing

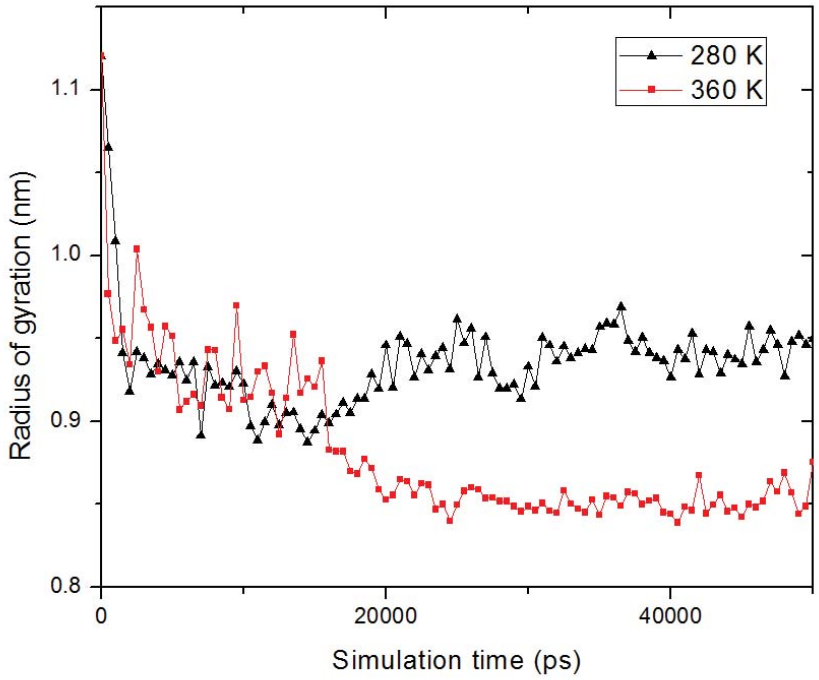

FIGURE 3.8: Radii of gyration at 280 K and 360 K, polyNAGA30 with Gasteiger charges along with AMBER force field and TIP3P water model

temperature which was opposite to the expected temperature dependence. At 280 K, the radius of gyration was 0.94 ± 0.01 nm. At 360 K, the radius of gyration was 0.85 ± 0.01 nm.

3.5 Conclusion

Compared to polyNAGA10 case, more variables were introduced into the simulation. Apart from the different charge assignments, the force field parameters and the water models were varied in an attempt to reproduce the upper critical solution temperature behavior of polyNAGA. Similar to polyNAGA10 system, the COMPASS charges, the OPLS-AA charges, the QEq charges and the Gasteiger charges were investigated. For the force field parameters, two different force fields were used, the OPLS-AA force field and the AMBER force field. The water models used were TIP4P, SPC/E and TIP3P. There was no significant difference between the radius of gyration value at 280 K and 360 K. With the attempt of trying different water models and charge assignment methods, the polyNAGA chain with 30 repeating units tended to adopt a collapse conformation. Using the AMBER force field along with the TIP3P water model generated the behavior which was not consistent with experiment.

Chapter 4

Multiple polyNAGA30 chains in water

In this Chapter, we reported the conformation of multiple polyNAGA chains each with 30 repeating units in water. Using multiple chains would allow us to study chain-chain interactions explicitly. An approach similar to that was used in the last two chapters was used except that the simulation unit cell was larger and more water molecules were needed to achieve a low concentration of polyNAGA.

4.1 Model construction of multiple polyNAGA30 chains

The cubic unit cell was constructed using the procedure described in Chapter 2. The polymer was built in a bulk density. The box was then expanded to large

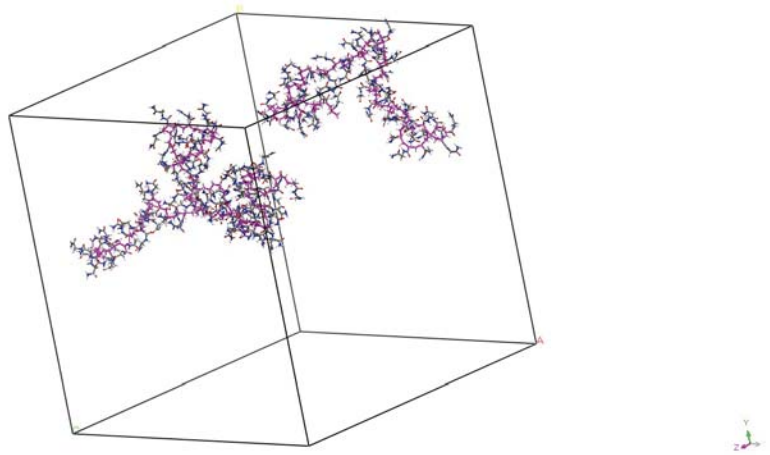

FIGURE 4.1: The structure of 5 polyNAGA30 chains in water, water molecules are not shown for clarity

enough for water. The resulting cubic cell had an edge length of 8 nm. In this case, the model could mimic the experiment situation that polyNAGA will form small aggregate even at very low concentration. However, 5 chains each with 30 repeating units were placed in the cubic unit cell. The five polyNAGA chains were placed in the cubic unit cell one by one in random locations in the simulation cell. The chains were placed in the simulation cell in such a manner that hard overlap of atoms from different chains was avoided. After that, water molecules were added and there were a total of 16,273 water molecules. The concentration of polyNAGA in this case was about about 6.18 wt%. Energy minimization was performed on the entire system before subsequent MD simulations were carried out on the system.

The number of hydrogen bonds is another measured quantity. Hydrogen bond is defined geometrically :(1) the cutoff radius between acceptor and donor is 0.35 nm. (2) the cut off angle of hygrogen - donor - acceptor is less than 30 degree.

For clarity, water molecules are not shown in the figure. The simulation time used was 100 ns simulation. Compared to the single chain system, this system required longer equilibration time.

4.2 Multiple polyNAGA30 chains with COMPASS charges

4.2.1 OPLS-AA force field and TIP4P water model

In this section, the COMPASS charges, OPLS-AA force field and TIP4P water model were used to describe the inter-molecular and intra-molecular interactions of the multiple-chain, polyNAGA solution model. The COMPASS charges were assigned to each atom when the model was built in the Materials Studio as the COMPASS force field is the default force field. And such charges were used in subsequent MD simulation even though the OPLS-AA force field was used. We used the TIP4P water model. To save computation time, only two temperatures (280 K and 360 K) were used. The pressure was set at 1 bar. The simulation time used was 100 ns simulation. Compared to the single chain system, this system required longer equilibration time.

Figure 4.2 shows radii of gyration of all five chains as a function of time calculated for each polymer chain. Generally, radii of gyration of the chains seemed to be insensitive to temperature. In other words, the use of COMPASS charges, OPLS-AA force field and TIP4P water model was not able to the experimentally observed

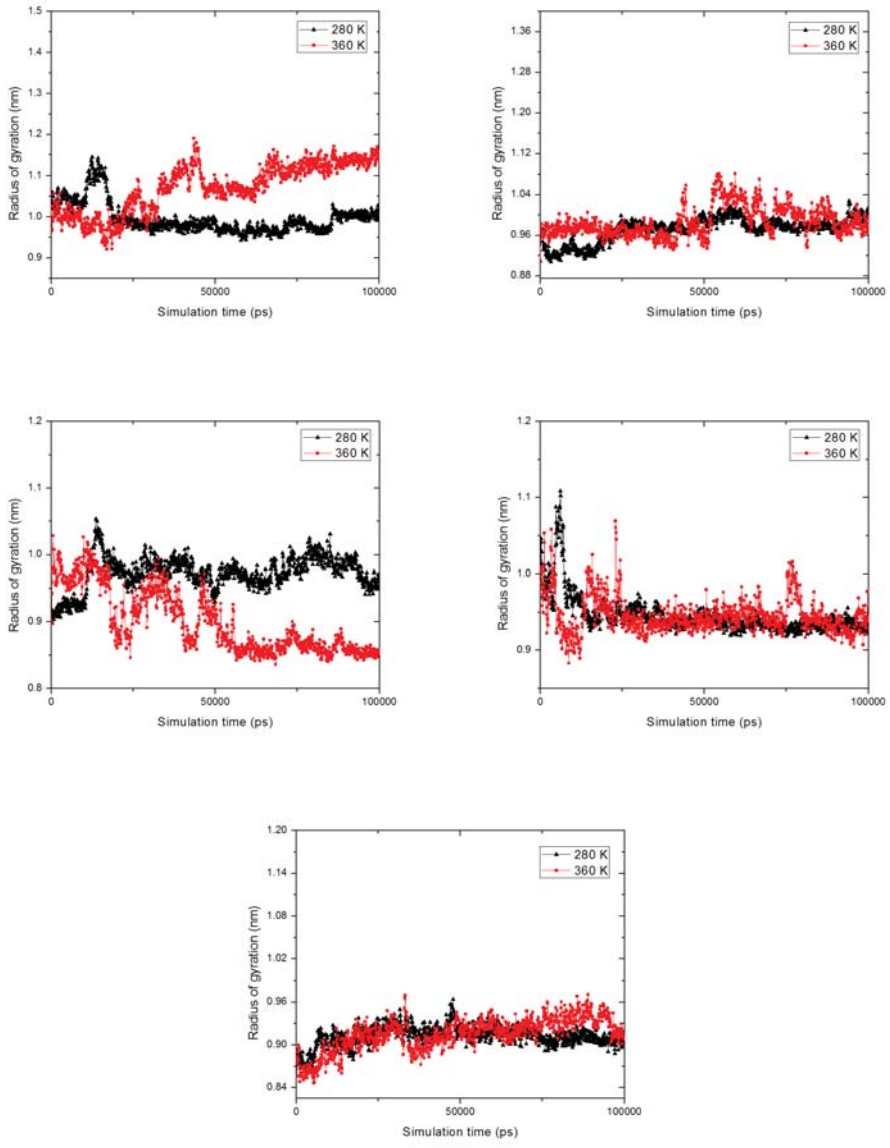

FIGURE 4.2: Five polyNAGA30 chains with COMPASS charges along with OPLS-AA force filed and the TIP4P water model

UCST behavior of the polyNAGA solution. At 360 K, the average radius of gyration of 5 chains was 0.97 $\pm$ 0.10 nm. At 280 K, the average radius of gyration of 5 chains was 0.96 $\pm$ 0.04 nm.

4.2.2 OPLS-AA force field and SPC/E water model

In this section, similar to what we did before, we used COMPASS charges and the OPLS-AA force field. However, the SPC/E water model was used in an attempt to determine the effect of water model on the calculated radii of gyration of polyNAGA.

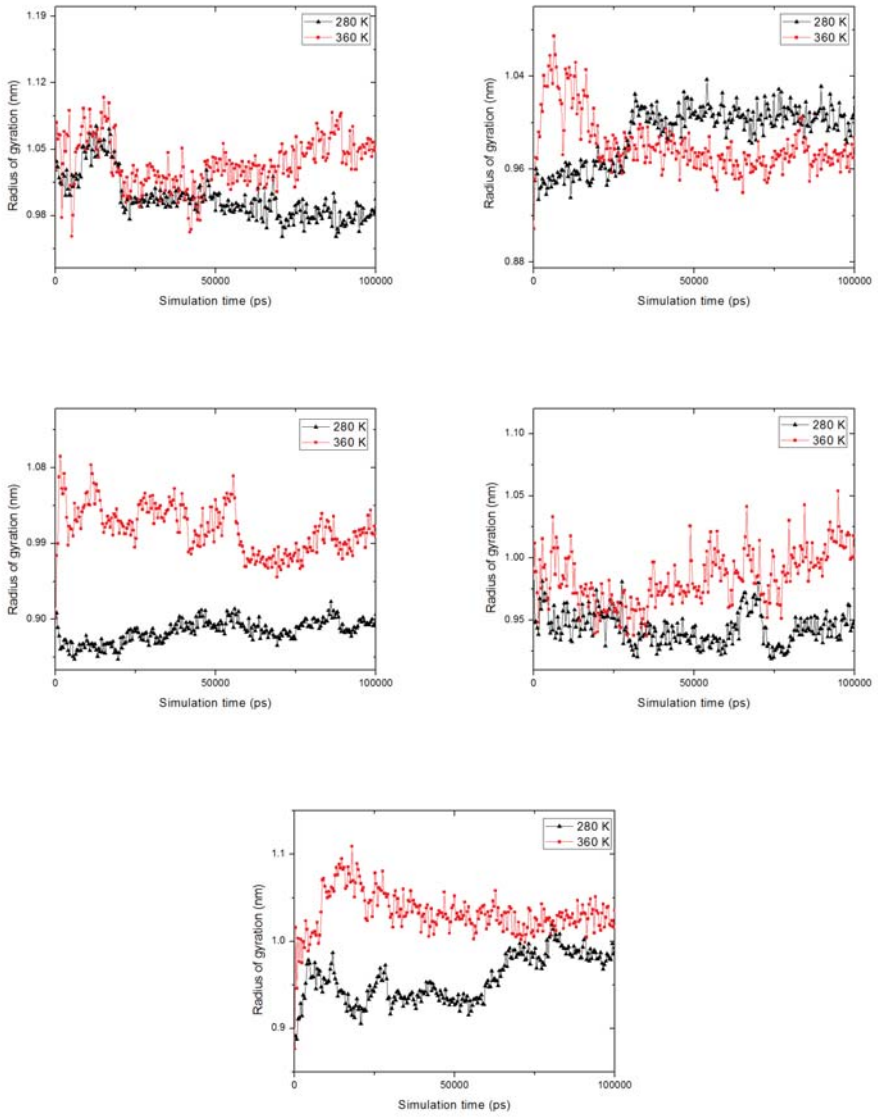

FIGURE 4.3: Five polyNAGA30 chains with COMPASS charges along with the OPLS-AA force filed and SPC/E water model

Figure 4.3, radii of gyration of 5 polymer chains at 280 K and 360 K are shown. At 280 K, the average radius of gyration of 5 chains was 0.96 ± 0.04 nm. In this case, 4 out of 5 chains exhibited much higher radius of gyration at 360 K. At 360 K, the average radius of gyration of 5 chains was 1.01 ± 0.03 nm. This suggested that the SPC/E water model was more suitable to describe the polyNAGA solution. In this case, we calculated numbers of different types of hydrogen bonds to investigate the mechanism. The SPC/E water model uses the theoretical hydrogen-oxygen-hydrogen bond angle 109.47 ° that is rare in the water model. For example, both TIP4P and TIP3P water models use a hydrogen-oxygen-hydrogen bond angle of 104.52° (experiment).

TABLE 4.1: Average number of polyNAGA30-water H-bonds

Chain	280 K	360 K
Chain 1	97±5	82±6
Chain 2	101±6	79±7
Chain 3	77±6	57±6
Chain 4	108±6	77±6
Chain 5	98±5	77±8

In Table 4.1, average numbers of hydrogen bonds formed between polyNAGA30 and water were shown. In this table, numbers of hydrogen bonds at 360K was generally lower than those at 280 K. It makes sense as the hydrogen bonds are easily broken due to the high thermal motion. In this way, the outer interaction of polymer with water becomes weak at high temperature.

In Table(4.2), average numbers of intermolecular hydrogen bonds of polyNAGA30 were depicted.

TABLE 4.2: Average numbers of intermolecular H-bonds of polyNAGA30

Chain	280 K	360 K
Chain 1	46±5	46±6
Chain 2	37±5	51±7
Chain 3	51±7	55±5
Chain 4	34±5	48±6
Chain 5	41±5	40±6

TABLE 4.3: Average number of intramolecular H-bonds of polyNAGA30

Chain	280 K	360 K
Chain 1	20±2	18±3
Chain 2	15±2	23±3
Chain 3	19±3	19±2
Chain 4	15±2	20±3
Chain 5	17±2	14±3

In Table 4.3, the average number of hydrogen bonds inside one polymer was calculated. So it seemed that, even though the OPLS-AA force field and SPC/E water model with COMPASS charges showed the UCST behavior. The data shown in Table 4.1,4.2,4.3 suggested that hydrogen bonds may not be the cause for the observation.

4.2.3 AMBER force field and TIP3P water model

In this section, the COMPASS charges, AMBER force field and TIP3P water model were used for the MD simulation at 280 K and 360 K. TIP3P was used as this is normally the water model suggested to use along with the AMBER force field. Comparing the AMBER to the OPLS-AA force field, they both use similar functions and parameters for calculating the bonded force and non-bonded interactions. For example, The Lennard-Jonnes parameters used in the two force fields describing the van der Waals interaction of the same type of atom are slightly different. The AMBER force field is specially designed for biomacromolecules. Since polyNAGA contains chemical moieties similar to amino acids, use of the AMBER force field should be justified.

Figure 4.4, radii of gyration of 5 polymer chains was calculated. At 280 K, the average radius of gyraiton of 5 chains was 0.97 ± 0.02 nm. At 360 K, the average radius of gyration of 5 chains was 0.98 ± 0.06 nm. Once again, similar to the results reported in the last section, the present results did not show that polyNAGA is a UCST polymer.

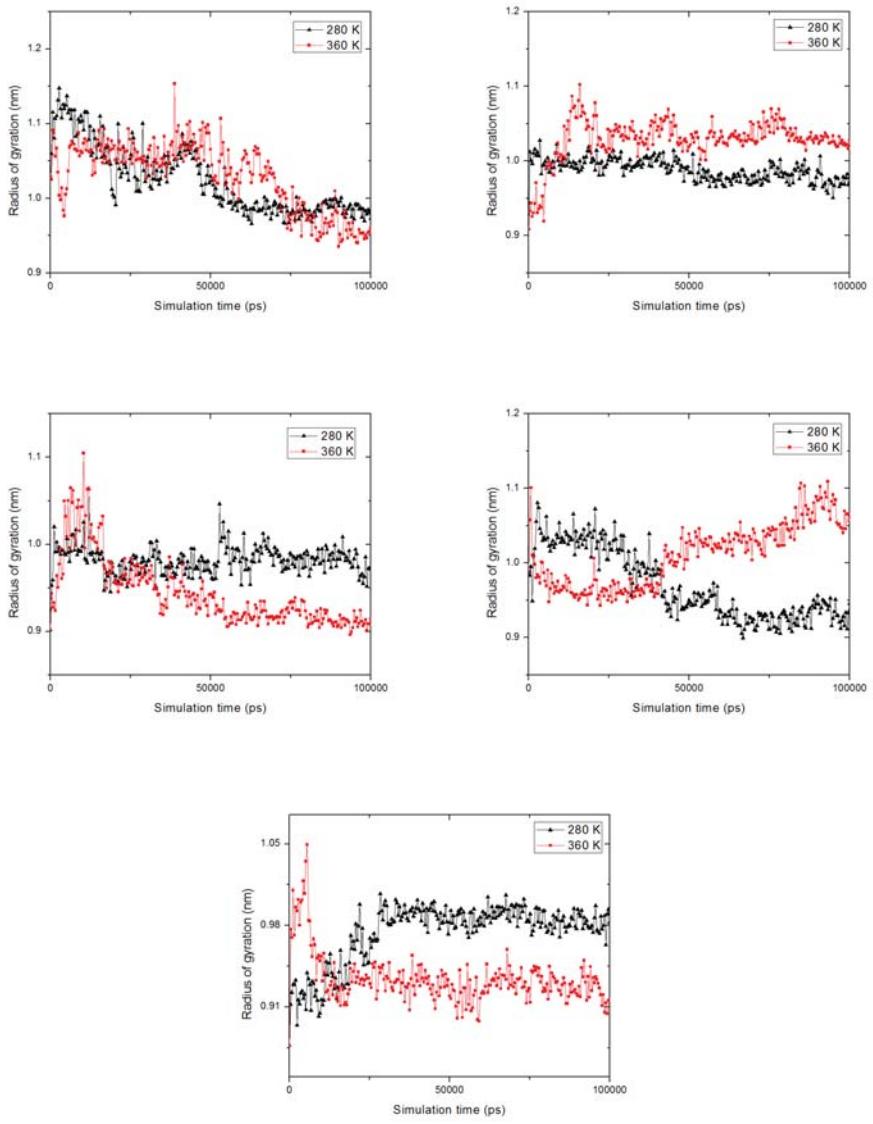

FIGURE 4.4: Five polyNAGA30 chains with COMPASS charges along with the AMBER force field and TIP3P water model

4.3 Mutilple polyNAGA30 chains with Gasterger charges

In this section, the Gasteiger charge method was used to assign partial atomic charges on polyNAGA. The OPLS-AA force field and SPC/E water model were used.

Figure 4.5 depicts the time dependence of the radius of gyration of all five polyNAGA chains at 280 K and 360 K. All five chains have the same trend that the radius of gyration at 360 K was larger than 280 K. It seemed that Gasteiger charges, OPLS-AA force field and SPC/E water model together yielded the expected results. At 280 K, the average radius of gyration of 5 chains was 0.89 $\pm$ 0.03 nm. At 360 K, the average radius of gyration of 5 chains was 1.01 $\pm$ 0.12 nm.

TABLE 4.4: Average number of polyNAGA30-water H-bond

Chain	280 K	360 K
Chain 1	32±4	27±4
Chain 2	40±4	32±5
Chain 3	24±3	18±4
Chain 4	30±4	22±4
Chain 5	37±5	27±4

Table 4.4 shows the average number of hydrogen bonds formed between polyNAGA30 and water. In this table, numbers of hydrogen bonds at 360 K was generally lower than those at 280 K. At 360 K, hydrogen bond was easily broken

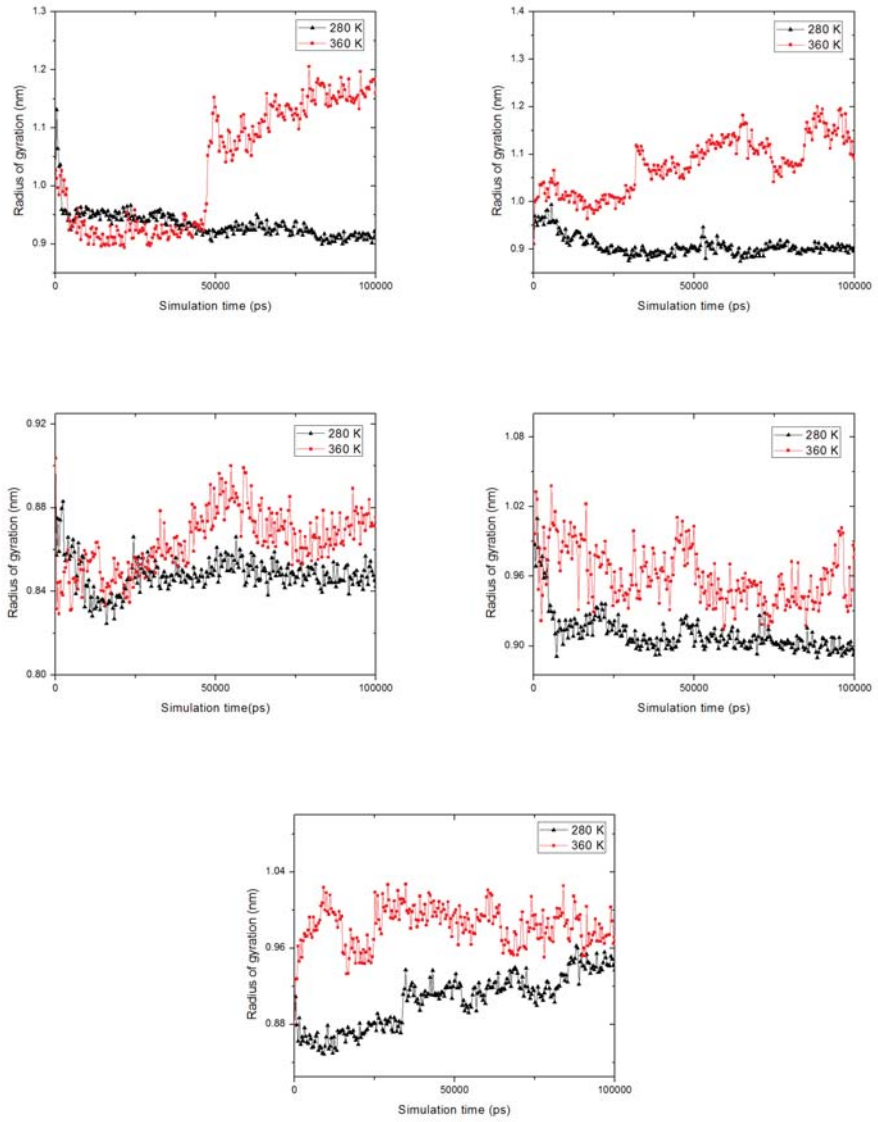

FIGURE 4.5: Five polyNAGA30 chains with Gasteiger charges along with the OPLS-AA force filed and SPC/E water model

due to the high thermal motion. In this way, the outer interaction of polymer with water became weak at high temperatures.

TABLE 4.5: Average number of intermolecular H-bonds of polyNAGA30

Chain	280 K	360 K
Chain 1	30±6	30±7
Chain 2	30±7	26±6
Chain 3	33±7	35±8
Chain 4	37±7	31±7
Chain 5	34±7	30±6

In Table(4.5) showed the average number of intermolecular hydrogen bonds of polyNAGA30. In this table, the number of hydrogen bonds at 280 K was larger than 360 K, which means the hydrogen bond interaction of polymer to polymer decreased. The average number of intermolecular H-bonds of total five chains at 280 K was 32.8 ± 2.9 and at 360 K was 30.4 ± 3.2. In this way, the decreasing of hydrogen bonds number would benefit the expansion of polymer chains.

TABLE 4.6: Average number of intramolecular H-bonds of polyNAGA30

Chain	280 K	360 K
Chain 1	11±2	11±3
Chain 2	13±3	9±2
Chain 3	12±3	13±3
Chain 4	14±3	11±3
Chain 5	13±3	10±3

In Table 4.6 showed the average number of intramolecular hydrogen bonds of polyNAGA30. That means the hydrogen bonds interaction between the side chains

on one polymer chain. The average number of intramolecular H-bonds of total five chains at 280 K was 12.6 ± 1.1 and at 360 K was 10.8 ± 1.4.

4.4 Conclusion

The computational cost for the simulation described in this Chapter was high.

Three water models were used, including the TIP4P, TIP3P and SPC/E. The OPLS-AA and AMBER force fields were used.

When the Gasteiger charges along with the OPLS-AA force field and SPC/E water model were used, all five chains exhibited UCST trends as supported by the radius of gyration at two different temperatures 280 K and 360 K. Then we calculated the three different types of hydrogen bonds. They were hydrogen bonds within one polymer chain, hydrogen bonds between polymer chains and hydrogen bonds between water and polymers.

The multiple chains system introduces the chain to chain interaction more explicitly. In this case, comparing with the single chain longer polyNAGA chain, the mutltiple chains are more realistic.

From what we observed, the Gasteiger charges were successful in reproducing the UCST behavior of polyNAGA in the multiple chain system. Combining with the result of short and single chain polyNAGA, in general, the Gasteiger charge assignment method is the most successful method to reproduce the UCST phenomenon. And, the UCST behavior is likely attributed to the decrease in the intramolecular hydrogen bonds upon heating.

Chapter 5

Conclusion

In this work, a water-soluble polymer poly(N-acryloyl glycinamide) (polyNAGA) that exhibits upper critical solution temperature (UCST) behavior was studied by molecular dynamics simulation. Most of polymers are not water-soluble polymers. Furthermore, it should be noted that majority of water-soluble polymers exhibit the so-called lower critical solution temeprature (LCST) behavior. In fact, it is unusual for polyNAGA, a non-ionic polymer, to exhibit the UCST behavior. Therefore, it is interesting to study the molecular mechanism that is responsible for such behavior. To determine the phase behavior of polyNAGA solution, we examined the conformation of polyNAGA in water over the temeprature range of 280 to 360 K using molecular dynamics simulation. Conformation of polyNAGA is quantified by calculating its radius of gyration in water at different temperatures over the aforementioned temperature range. Here, an expanded conformation (larger radius of gyration) signifies solubility while a contracted conformation (smaller radius of gyration) indicates possibility of precipitation.

To simulate the polyNAGA solutions, we used single and multiple chain models along with different force fields, partial atomic charge assignment methods and water models. The simulation results showed that the Gasteiger method is more suitable to be used than other methods such as charge equilibration method or OPLS charges as the Gasteiger method reproduced the UCST behavior of polyNAGA. In addition, the multiple chain model is better than the single chain model as the latter does not capture the intermolecular interactions between polyNAGA molecules effectively. In fact, it is experimentally observed that polyNAGA chains interact with each other even under extremely dilution situation.

5.1 Effect of partial atomic charges on the conformation of a single polyNAGA10 chain in water

We used a model containing a single polyNAGA chain with 10 repeating units surrounded by 2,109 water molecules. The OPLS-AA and AMBER force fields were used. However, we used four different methods including the charge equilibration, COMPASS, Gastiger and OPLS to assign partial atomic charges to polyNAGA molecule. The water model used was TIP4P. It was found that the Gasteiger method reproduced the UCST behavior while the other methods did not. In particular, the radius of gyration of polyNAGA increases from 0.56 nm $\pm$ 0.01 at 280 K to 0.65 nm $\pm$ 0.04 at 360 K gradually. Furthermore, the data do not show an abrupt change over the temeperatue range used for the simulations, making

identifying a unique UCST difficult. Also, it was found that the number of hydrogen bonds fromed between poly(NAGA) and water molecuels increased with increasing temperature while the intra-molecular hydrogen bonds of poly(NAGA) decreased with increasing temperature. The hydrogen bond data are consistent with the radius of gyration observation.

5.2 Conformation of a single polyNAGA30 chain in water

In this work, a longer polyNAGA chain with 30 repeating units was used in the molecular dynamics simulations. Similar to the work mentioned in the previous section, we also used different force fields, partial charge assignments methods, and water models to model the system. Radii of gyration of the system at different temperatures were calculated. We used the OPLS-AA and AMBER force fields. Different water models combined with different force fields and different partial charge assignment are attempted to reproduce the UCST behavior. For the polyNAGA with 30 repeating units, we were not able to identify a combination of force field, partial atomic charge assignment method and water model to reproduce the UCST behavior of polyNAGA solution. In most cases, the polyNAGA chain adopted a fairly compact conformation at different tempratures. The reason for the long, single polyNAGA chain not exhibiting the UCST behavior is unclear.

5.3 Multiple polyNAGA30 chains in water

The multiple polyNAGA chain model with 30 repeat units system was used to continue the analysis. In this section, the intermolecular interaction between polyNAGA chains was explicitly introduced. Similar to the single chain model, different partial atomic charge assignments, different force fields and different water models are used. It seems that Gasteiger charges along with OPLS-AA force field and SPCE water model was able to reproduce the UCST. Then we calculate the three different types of hydrogen bonds. They are hydrogen bonds within one polymer chain, hydrogen bonds between polymer chains and hydrogen bonds between water and polymers. The hydrogen bonds between polymers decreased with increasing temperature. That means, with increasing temperature, the polymer expands. The hydrogen bonds between polymer and water decreased with increasing temperature because the high thermal motion will break the hydrogen bonds. So in general, the Gasteiger charges assignment are also successful in reproducing the USCT phenomena on the multiple chain model.

5.4 Further work

The work reported in this thesis signifies the first attempt to study the molecular mechanism that is responsible for the experimentally observed UCST behavior of polyNAGA in water. The partial atomic charges and water model play important roles in determining the phase behavior of polyNAGA solution as the electrostactic interactions determine the number of intra-molecular hydrogen bonds

of polyNAGA and intermolecular hydrogen bonds between polyNAGA and water at different temperatures. The further work can go into three directions. The first direction is to determine partial atomic charges using first principle quantum mechanical calcualtions along with different population analysis methods. This may allow us to identify a sharper UCST for polyNAGA. We also want to do the torsion angle analysis. We will examine the influence of the partial atomic charges on the torsion potentials of the skeletal bonds in polyNAGA once we have determined a more accurate way of assigning charges. Obviously, the torsion potentials will affect the conformation of polyNAGA in water. The other direction is to carry out further MD calculations on new hypothetical, water-soluble polymers similar to polyNAGA with modified side chains. The side chains in polyNAGA are very unique with many hydrogen donors and acceptors. Changing the function groups on the side chains will definitely alter the solubility behavior of polyNAGA. The final direction is to carry out MD study on the interaction between polymers and clay surfaces to determine the potential of using such water-soluble, UCST polymers as a flocculant in the oil sands tailings treatment.

Bibliography

[1] Jan Seuring and Seema Agarwal. Polymers with upper critical solution temperature in aqueous solution: Unexpected properties from known building blocks. *ACS Macro Letters*, 2(7):597–600, 2013.

[2] Suk Yung Oh and Young Chan Bae. Role of intermolecular interactions for upper and lower critical solution temperature behaviors in polymer solutions: Molecular simulations and thermodynamic modeling. *Polymer*, 53 (17):3772–3779, 2012.

[3] Yoshinori Tamai, Hideki Tanaka, and Koichiro Nakanishi. Molecular dynamics study of water in hydrogels. *Molecular Simulation*, 16(4-6): 359–374, 1996.

[4] Yasushi Maeda, Noriaki Tsukida, Hiromi Kitano, Takahiko Terada, and Junpei Yamanaka. Raman spectroscopic study of water in aqueous polymer solutions. *The Journal of Physical Chemistry*, 97(51):13903–13906, 1993.

[5] Seung Geol Lee, Tod A Pascal, Wonsang Koh, Giuseppe F Brunello, William A Goddard III, and Seung Soon Jang. Deswelling mechanisms of

surface-grafted poly (nipaam) brush: Molecular dynamics simulation approach. *The Journal of Physical Chemistry C*, 116(30):15974–15985, 2012.

[6] M. L. Huggins. Solutions of long chain compounds. *jcp*, 9:440, 1941.

[7] Maurice L. Huggins. Theory of solutions of high polymers1. *Journal of the American Chemical Society*, 64(7):1712–1719, 1942.

[8] P J Flory and W R Krigbaum. Thermodynamics of high polymer solutions. *Annual Review of Physical Chemistry*, 2(1):383–402, 1951.

[9] Fangyao Liu, Jan Seuring, and Seema Agarwal. Controlled radical polymerization of n-acryloylglycinamide and ucst-type phase transition of the polymers. *Journal of Polymer Science Part A: Polymer Chemistry*, 50 (23):4920–4928, 2012.

[10] Charles L. McCormick Andrew B.Lowe. Synthesis and solution properties of zwitterionic polymers. *Chem. Rev*, pages 4177–4189, 2002.

[11] Pascaline Mary, Denis D. Bendejacq, Marie-Pierre Labeau, and Patrick Dupuis. Reconciling low- and high-salt solution behavior of sulfobetaine polyzwitterions. *The Journal of Physical Chemistry B*, 111(27):7767–7777, 2007.

[12] Peter Köberle, André Laschewsky, and Terence D. Lomax. Interactions of a zwitterionic polysoap and its cationic analog with inorganic salts. *Die Makromolekulare Chemie, Rapid Communications*, 12(7):427–433, 1991.

[13] Jan Seuring, Frank M. Bayer, Klaus Huber, and Seema Agarwal. Upper critical solution temperature of poly(n-acryloyl glycinamide) in water: A concealed property. *Macromolecules*, 45(1):374–384, 2012.

[14] Jan Seuring and Seema Agarwal. Non-ionic homo- and copolymers with h-donor and h-acceptor units with an ucst in water. *Macromolecular Chemistry and Physics*, 211(19):2109–2117, 2010.

[15] Yoshinori Tamai, Hideki Tanaka, and Koichiro Nakanishi. Molecular dynamics study of polymer-water interaction in hydrogels. 1. hydrogen-bond structure. *Macromolecules*, 29(21):6750–6760, 1996.

[16] Yoshinori Tamai, Hideki Tanaka, and Koichiro Nakanishi. Molecular dynamics study of polymer-water interaction in hydrogels. 2. hydrogen-bond dynamics. *Macromolecules*, 29(21):6761–6769, 1996.

[17] Mohammad Alaghemandi and Eckhard Spohr. Molecular dynamics investigation of the thermo-responsive polymer poly(n-isopropylacrylamide). *Macromolecular Theory and Simulations*, 21(2):106–112, 2012.

[18] Hongbo Du and Xianghong Qian. Molecular dynamics simulations of pnipam-co-pegma copolymer hydrophilic to hydrophobic transition in nacl solution. *Journal of Polymer Science Part B: Polymer Physics*, 49(15): 1112–1122, 2011.

[19] Sriram Srikant, Sulatha S. Muralidharan, and Upendra Natarajan. Behaviour of hydrogen bonding and structure of poly(acrylic acid) in

water–ethanol solution investigated by explicit ion molecular dynamics simulations. *Molecular Simulation*, 39(2):145–153, 2013.

[20] Fabrizio Gangemi, Giovanna Longhi, Sergio Abbate, France Lebon, Roberto Cordone, Gian Paolo Ghilardi, and Sandro L Fornili. Molecular dynamics simulation of aqueous solutions of 26-unit segments of p (nipaam) and of p (nipaam)"doped" with amino acid based comonomers. *The Journal of Physical Chemistry B*, 112(38):11896–11906, 2008.

[21] Paulo A Netz and Thomas Dorfmüller. Computer simulation studies on the polymer-induced modification of water properties in polyacrylamide hydrogels. *The Journal of Physical Chemistry B*, 102(25):4875–4886, 1998.

[22] David S Simmons and Isaac C Sanchez. Scaled particle theory for the coil–globule transition of an isolated polymer chain. *Macromolecules*, 46 (11):4691–4697, 2013.

[23] Pekka Mark and Lennart Nilsson. Structure and dynamics of the tip3p, spc, and spc/e water models at 298 k. *The Journal of Physical Chemistry A*, 105 (43):9954–9960, 2001.

[24] T. Darden, D. York, and L. Pedersen. Particle mesh Ewald: An N . log(N) method for Ewald sums in large systems. *jcp*, 98:10089–10092, jun 1993.

[25] Ulrich Essmann, Lalith Perera, Max L. Berkowitz, Tom Darden, Hsing Lee, and Lee G. Pedersen. A smooth particle mesh ewald method. *The Journal of Chemical Physics*, 103(19):8577–8593, nov 1995.

[26] Huai Sun. Compass: An ab initio force-field optimized for condensed-phase applications overview with details on alkane and benzene compounds. *The Journal of Physical Chemistry B*, 102(38):7338–7364, 1998.

[27] William L Jorgensen, David S Maxwell, and Julian Tirado-Rives. Development and testing of the opls all-atom force field on conformational energetics and properties of organic liquids. *Journal of the American Chemical Society*, 118(45):11225–11236, 1996.

[28] Marsili M Gasteiger, J. New model for calculating atomic charges in moleculars. *TETRAHEDRON LETTERS*, 34:3181–3184, 1978.

[29] Anthony K Rappe and William A Goddard III. Charge equilibration for molecular dynamics simulations. *The Journal of Physical Chemistry*, 95(8): 3358–3363, 1991.

[30] Min Zhang and René Fournier. Self-consistent charge equilibration method and its application to au13na n (n= 1, 10) clusters. *The Journal of Physical Chemistry A*, 113(13):3162–3170, 2009.

[31] J. D. Bernal and R. H. Fowler. A theory of water and ionic solution, with particular reference to hydrogen and hydroxyl ions. *The Journal of Chemical Physics*, 1(8):515–548, 1933.

[32] William L. Jorgensen, Jayaraman Chandrasekhar, Jeffry D. Madura, Roger W. Impey, and Michael L. Klein. Comparison of simple potential functions for simulating liquid water. *The Journal of Chemical Physics*, 79 (2):926–935, 1983.

[33] Michael W. Mahoney and William L. Jorgensen. A five-site model for liquid water and the reproduction of the density anomaly by rigid, nonpolarizable potential functions. *The Journal of Chemical Physics*, 112(20):8910–8922, 2000.

[34] Michael W Mahoney and William L Jorgensen. Diffusion constant of the tip5p model of liquid water. *The Journal of Chemical Physics*, 114(1): 363–366, 2001.

[35] William L Jorgensen and Corky Jenson. Temperature dependence of tip3p, spc, and tip4p water from npt monte carlo simulations: Seeking temperatures of maximum density. *Journal of computational chemistry*, 19 (10):1179–1186, 1998.

[36] Peter G Kusalik and Igor M Svishchev. The spatial structure in liquid water. *Science*, 265(5176):1219–1221, 1994.

[37] Yujie Wu, Harald L Tepper, and Gregory A Voth. Flexible simple point-charge water model with improved liquid-state properties. *The Journal of chemical physics*, 124(2):024503, 2006.

[38] Philippe H. Hünenberger. *Thermostat Algorithms for Molecular Dynamics Simulations*. 2005.

[39] Pekka Mark and Lennart Nilsson. Structure and dynamics of the tip3p, spc, and spc/e water models at 298 k. *The Journal of Physical Chemistry A*, 105 (43):9954–9960, 2001.

[40] Jonathan Walter, Viktor Ermatchkov, Jadran Vrabec, and Hans Hasse. Molecular dynamics and experimental study of conformation change of poly (n-isopropylacrylamide) hydrogels in water. *Fluid Phase Equilibria*, 296(2): 164–172, 2010.

PDB file of polyNAGA10

ATOM	1	C1	C6	P	0	5.879	6.555	8.756	1.00	0.00	C
ATOM	2	C2	C6	P	0	4.974	6.461	10.026	1.00	0.00	C
ATOM	3	O3	C6	P	0	4.138	5.585	10.177	1.00	0.00	O
ATOM	4	N4	C6	P	0	5.162	7.411	10.962	1.00	0.00	N
ATOM	5	C5	C6	P	0	4.422	7.321	12.232	1.00	0.00	C
ATOM	6	C6	C6	P	0	3.028	7.943	12.073	1.00	0.00	C
ATOM	7	O7	C6	P	0	2.747	9.089	12.372	1.00	0.00	O
ATOM	8	N8	C6	P	0	2.119	7.092	11.567	1.00	0.00	N
ATOM	9	C9	C6	P	0	5.300	5.564	7.726	1.00	0.00	C
ATOM	10	H1	0 C6	P	0	5.831	7.566	8.314	1.00	0.00	H
ATOM	11	H1	1 C6	P	0	5.889	8.100	10.883	1.00	0.00	H
ATOM	12	H1	2 C6	P	0	4.911	7.979	12.961	1.00	0.00	H
ATOM	13	H1	3 C6	P	0	4.440	6.298	12.640	1.00	0.00	H
ATOM	14	H1	4 C6	P	0	1.169	7.401	11.447	1.00	0.00	H
ATOM	15	H1	5 C6	P	0	2.432	6.194	11.233	1.00	0.00	H
ATOM	16	C1	6 C6	P	0	7.334	6.223	9.167	1.00	0.00	C
ATOM	17	H1	7 C6	P	0	7.299	5.315	9.800	1.00	0.00	H
ATOM	18	H1	8 C6	P	0	7.724	7.024	9.815	1.00	0.00	H
ATOM	19	H1	9 C6	P	0	5.849	5.629	6.773	1.00	0.00	H
ATOM	20	H2	0 C6	P	0	4.244	5.786	7.505	1.00	0.00	H
ATOM	21	H2	1 C6	P	0	5.373	4.524	8.082	1.00	0.00	H
ATOM	22	C2	2 C5	P	0	8.350	5.874	8.052	1.00	0.00	C
ATOM	23	C2	3 C5	P	0	8.436	6.749	6.798	1.00	0.00	C
ATOM	24	O2	4 C5	P	0	8.385	6.232	5.692	1.00	0.00	O
ATOM	25	N2	5 C5	P	0	8.461	8.096	6.916	1.00	0.00	N
ATOM	26	C2	6 C5	P	0	9.014	8.914	8.003	1.00	0.00	C
ATOM	27	C2	7 C5	P	0	10.419	9.509	7.833	1.00	0.00	C
ATOM	28	O2	8 C5	P	0	10.892	10.239	8.690	1.00	0.00	O
ATOM	29	N2	9 C5	P	0	11.165	9.208	6.754	1.00	0.00	N
ATOM	30	H3	0 C5	P	0	7.957	4.955	7.586	1.00	0.00	H
ATOM	31	H3	1 C5	P	0	8.445	8.582	6.024	1.00	0.00	H
ATOM	32	H3	2 C5	P	0	9.075	8.333	8.928	1.00	0.00	H
ATOM	33	H3	3 C5	P	0	8.362	9.784	8.174	1.00	0.00	H
ATOM	34	H3	4 C5	P	0	10.811	8.671	5.981	1.00	0.00	H
ATOM	35	H3	5 C5	P	0	12.047	9.684	6.677	1.00	0.00	H

ATOM	36	C3	6 C5	P	0	9.724	5.513	8.688	1.00	0.00	C
ATOM	37	H3	7 C5	P	0	9.488	4.866	9.555	1.00	0.00	H
ATOM	38	H3	8 C5	P	0	10.191	6.417	9.117	1.00	0.00	H
ATOM	39	C3	9 C5	P	0	10.808	4.781	7.852	1.00	0.00	C
ATOM	40	C4	0 C5	P	0	10.267	3.471	7.297	1.00	0.00	C
ATOM	41	O4	1 C5	P	0	10.465	2.417	7.883	1.00	0.00	O
ATOM	42	N4	2 C5	P	0	9.558	3.501	6.152	1.00	0.00	N
ATOM	43	C4	3 C5	P	0	8.920	2.261	5.680	1.00	0.00	C
ATOM	44	C4	4 C5	P	0	7.557	2.066	6.358	1.00	0.00	C
ATOM	45	O4	5 C5	P	0	6.526	2.593	5.982	1.00	0.00	O
ATOM	46	N4	6 C5	P	0	7.574	1.237	7.417	1.00	0.00	N
ATOM	47	H4	7 C5	P	0	11.549	4.396	8.571	1.00	0.00	H
ATOM	48	H4	8 C5	P	0	9.196	4.374	5.795	1.00	0.00	H
ATOM	49	H4	9 C5	P	0	9.621	1.414	5.734	1.00	0.00	H
ATOM	50	H5	0 C5	P	0	8.647	2.401	4.629	1.00	0.00	H
ATOM	51	H5	1 C5	P	0	8.450	0.965	7.826	1.00	0.00	H
ATOM	52	H5	2 C5	P	0	6.708	1.151	7.931	1.00	0.00	H
ATOM	53	C5	3 C5	P	0	11.538	5.733	6.880	1.00	0.00	C
ATOM	54	H5	4 C5	P	0	12.114	6.433	7.514	1.00	0.00	H
ATOM	55	H5	5 C5	P	0	10.784	6.340	6.362	1.00	0.00	H
ATOM	56	C5	6 C5	P	0	12.484	5.150	5.791	1.00	0.00	C
ATOM	57	C5	7 C5	P	0	12.907	6.327	4.986	1.00	0.00	C
ATOM	58	O5	8 C5	P	0	12.091	7.140	4.565	1.00	0.00	O
ATOM	59	N5	9 C5	P	0	14.219	6.502	4.755	1.00	0.00	N
ATOM	60	C6	0 C5	P	0	14.678	7.653	3.961	1.00	0.00	C
ATOM	61	C6	1 C5	P	0	14.383	7.414	2.479	1.00	0.00	C
ATOM	62	O6	2 C5	P	0	14.817	6.467	1.849	1.00	0.00	O
ATOM	63	N6	3 C5	P	0	13.604	8.329	1.877	1.00	0.00	N
ATOM	64	H6	4 C5	P	0	11.849	4.603	5.071	1.00	0.00	H
ATOM	65	H6	5 C5	P	0	14.905	5.789	4.966	1.00	0.00	H
ATOM	66	H6	6 C5	P	0	15.777	7.679	4.009	1.00	0.00	H
ATOM	67	H6	7 C5	P	0	14.298	8.592	4.393	1.00	0.00	H
ATOM	68	H6	8 C5	P	0	13.397	8.177	0.903	1.00	0.00	H
ATOM	69	H6	9 C5	P	0	13.261	9.151	2.345	1.00	0.00	H
ATOM	70	C7	0 C5	P	0	13.543	4.174	6.355	1.00	0.00	C
ATOM	71	H7	1 C5	P	0	13.059	3.574	7.145	1.00	0.00	H
ATOM	72	H7	2 C5	P	0	14.309	4.767	6.888	1.00	0.00	H
ATOM	73	C7	3 C5	P	0	14.168	3.211	5.298	1.00	0.00	C
ATOM	74	C7	4 C5	P	0	15.652	3.255	5.510	1.00	0.00	C
ATOM	75	O7	5 C5	P	0	16.248	4.231	5.089	1.00	0.00	O
ATOM	76	N7	6 C5	P	0	16.335	2.235	6.119	1.00	0.00	N
ATOM	77	C7	7 C5	P	0	15.818	1.781	7.415	1.00	0.00	C
ATOM	78	C7	8 C5	P	0	16.725	0.698	8.010	1.00	0.00	C
ATOM	79	O7	9 C5	P	0	17.813	0.913	8.509	1.00	0.00	O
ATOM	80	N8	0 C5	P	0	16.214	-0.547	8.002	1.00	0.00	N

ATOM	81	H8	1 C5	P	0	14.138	3.716	4.316	1.00	0.00	H
ATOM	82	H8	2 C5	P	0	17.335	2.431	6.134	1.00	0.00	H
ATOM	83	H8	3 C5	P	0	14.767	1.479	7.328	1.00	0.00	H
ATOM	84	H8	4 C5	P	0	15.872	2.582	8.171	1.00	0.00	H
ATOM	85	H8	5 C5	P	0	15.414	-0.766	7.426	1.00	0.00	H
ATOM	86	H8	6 C5	P	0	16.814	-1.278	8.341	1.00	0.00	H
ATOM	87	C8	7 C5	P	0	13.251	1.963	5.200	1.00	0.00	C
ATOM	88	H8	8 C5	P	0	12.276	2.389	4.892	1.00	0.00	H
ATOM	89	H8	9 C5	P	0	13.066	1.554	6.209	1.00	0.00	H
ATOM	90	C9	0 C5	P	0	13.487	0.746	4.256	1.00	0.00	C
ATOM	91	C9	1 C5	P	0	14.606	-0.131	4.733	1.00	0.00	C
ATOM	92	O9	2 C5	P	0	14.473	-0.869	5.699	1.00	0.00	O
ATOM	93	N9	3 C5	P	0	15.749	-0.102	4.026	1.00	0.00	N
ATOM	94	C9	4 C5	P	0	16.864	-1.037	4.256	1.00	0.00	C
ATOM	95	C9	5 C5	P	0	17.008	-2.176	3.235	1.00	0.00	C
ATOM	96	O9	6 C5	P	0	17.966	-2.933	3.252	1.00	0.00	O
ATOM	97	N9	7 C5	P	0	16.049	-2.334	2.301	1.00	0.00	N
ATOM	98	H9	8 C5	P	0	12.638	0.077	4.478	1.00	0.00	H
ATOM	99	H9	9 C5	P	0	15.877	0.575	3.293	1.00	0.00	H
ATOM	100	0H1	0 C5	P	0	16.765	-1.519	5.237	1.00	0.00	H
ATOM	101	1H1	0 C5	P	0	17.824	-0.499	4.222	1.00	0.00	H
ATOM	102	2H1	0 C5	P	0	16.179	-3.048	1.600	1.00	0.00	H
ATOM	103	3H1	0 C5	P	0	15.219	-1.766	2.293	1.00	0.00	H
ATOM	104	C1	0 C5	P	0	13.474	1.094	2.739	1.00	0.00	C
ATOM	105	5H1	0 C5	P	0	14.316	0.624	2.202	1.00	0.00	H
ATOM	106	6H1	0 C5	P	0	13.633	2.177	2.586	1.00	0.00	H
ATOM	107	C1	0 C5	P	0	12.193	0.677	1.966	1.00	0.00	C
ATOM	108	C1	0 C5	P	0	11.917	-0.765	2.218	1.00	0.00	C
ATOM	109	O1	0 C5	P	0	12.803	-1.604	2.100	1.00	0.00	O
ATOM	110	N1	1 C5	P	0	10.680	-1.122	2.629	1.00	0.00	N
ATOM	112	C1	1 C5	P	0	9.083	-2.808	3.488	1.00	0.00	C
ATOM	113	O1	1 C5	P	0	8.978	-2.865	4.699	1.00	0.00	O
ATOM	114	N1	1 C5	P	0	8.016	-3.040	2.696	1.00	0.00	N
ATOM	115	5H1	1 C5	P	0	12.508	0.642	0.911	1.00	0.00	H
ATOM	116	6H1	1 C5	P	0	9.907	-0.479	2.654	1.00	0.00	H
ATOM	117	7H1	1 C5	P	0	11.139	-2.999	3.459	1.00	0.00	H
ATOM	118	8H1	1 C5	P	0	10.513	-3.087	1.796	1.00	0.00	H
ATOM	119	9H1	1 C5	P	0	8.060	-2.815	1.711	1.00	0.00	H
ATOM	120	0H1	2 C5	P	0	7.107	-3.037	3.143	1.00	0.00	H
ATOM	121	C1	2 C5	P	0	11.102	1.758	2.082	1.00	0.00	C
ATOM	122	2H1	2 C5	P	0	11.626	2.722	1.953	1.00	0.00	H
ATOM	123	3H1	2 C5	P	0	10.741	1.754	3.127	1.00	0.00	H
ATOM	124	C1	2 C5	P	0	9.896	1.671	1.106	1.00	0.00	C
ATOM	125	C1	2 C5	P	0	8.647	2.040	1.894	1.00	0.00	C
ATOM	126	O1	2 C5	P	0	7.952	1.160	2.366	1.00	0.00	O

ATOM	127	N1	2 C5	P	0	8.273	3.351	2.011	1.00	0.00	N
ATOM	128	C1	2 C5	P	0	9.248	4.425	2.295	1.00	0.00	C
ATOM	129	C1	2 C5	P	0	8.739	5.776	1.769	1.00	0.00	C
ATOM	130	O1	3 C5	P	0	8.728	6.088	0.592	1.00	0.00	O
ATOM	131	N1	3 C5	P	0	8.329	6.644	2.711	1.00	0.00	N
ATOM	132	2H1	3 C5	P	0	9.678	0.614	0.906	1.00	0.00	H
ATOM	133	3H1	3 C5	P	0	7.391	3.453	2.497	1.00	0.00	H
ATOM	134	4H1	3 C5	P	0	10.136	4.275	1.672	1.00	0.00	H
ATOM	135	5H1	3 C5	P	0	9.586	4.431	3.345	1.00	0.00	H
ATOM	136	6H1	3 C5	P	0	8.310	6.421	3.694	1.00	0.00	H
ATOM	137	7H1	3 C5	P	0	7.996	7.540	2.393	1.00	0.00	H
ATOM	138	C1	3 C5	P	0	10.023	2.433	-0.244	1.00	0.00	C
ATOM	139	9H1	3 C5	P	0	10.706	3.288	-0.132	1.00	0.00	H
ATOM	140	0H1	4 C5	P	0	9.046	2.891	-0.496	1.00	0.00	H
ATOM	141	C1	4 C5	P	0	10.401	1.651	-1.529	1.00	0.00	C
ATOM	142	C1	4 C5	P	0	11.760	0.915	-1.461	1.00	0.00	C
ATOM	143	O1	4 C5	P	0	11.883	-0.290	-1.380	1.00	0.00	O
ATOM	144	N1	4 C5	P	0	12.838	1.698	-1.662	1.00	0.00	N
ATOM	145	C1	4 C5	P	0	13.004	3.165	-1.633	1.00	0.00	C
ATOM	146	C1	4 C5	P	0	13.649	3.624	-0.327	1.00	0.00	C
ATOM	147	O1	4 C5	P	0	14.581	3.039	0.193	1.00	0.00	O
ATOM	148	N1	4 C5	P	0	13.133	4.741	0.220	1.00	0.00	N
ATOM	149	9H1	4 C5	P	0	10.467	2.404	-2.340	1.00	0.00	H
ATOM	150	0H1	5 C5	P	0	13.709	1.194	-1.571	1.00	0.00	H
ATOM	151	1H1	5 C5	P	0	12.053	3.652	-1.884	1.00	0.00	H
ATOM	152	2H1	5 C5	P	0	13.729	3.434	-2.420	1.00	0.00	H
ATOM	153	3H1	5 C5	P	0	13.695	5.144	0.963	1.00	0.00	H
ATOM	154	4H1	5 C5	P	0	12.488	5.338	-0.268	1.00	0.00	H
ATOM	155	C1	5 C5	P	0	9.274	0.723	-2.087	1.00	0.00	C
ATOM	156	6H1	5 C5	P	0	9.640	0.304	-3.043	1.00	0.00	H
ATOM	157	7H1	5 C5	P	0	8.479	1.443	-2.372	1.00	0.00	H
ATOM	158	C1	5 C5	P	0	8.472	-0.374	-1.339	1.00	0.00	C
ATOM	159	C1	5 C5	P	0	8.940	-1.715	-0.881	1.00	0.00	C
ATOM	160	O1	6 C5	P	0	8.269	-2.324	-0.056	1.00	0.00	O
ATOM	161	N1	6 C5	P	0	10.007	-2.299	-1.452	1.00	0.00	N
ATOM	162	C1	6 C5	P	0	10.358	-3.696	-1.132	1.00	0.00	C
ATOM	163	C1	6 C5	P	0	11.847	-4.036	-0.996	1.00	0.00	C
ATOM	164	O1	6 C5	P	0	12.225	-5.190	-0.856	1.00	0.00	O
ATOM	165	N1	6 C5	P	0	12.753	-3.042	-1.016	1.00	0.00	N
ATOM	166	6H1	6 C5	P	0	8.081	0.034	-0.393	1.00	0.00	H
ATOM	167	7H1	6 C5	P	0	10.546	-1.835	-2.171	1.00	0.00	H
ATOM	168	8H1	6 C5	P	0	9.990	-4.397	-1.895	1.00	0.00	H
ATOM	169	9H1	6 C5	P	0	9.924	-3.988	-0.165	1.00	0.00	H
ATOM	170	0H1	7 C5	P	0	13.733	-3.259	-0.907	1.00	0.00	H
ATOM	171	1H1	7 C5	P	0	12.461	-2.078	-1.083	1.00	0.00	H

ATOM	172	C1	7 C5	P	0	7.225	-0.662	-2.226	1.00	0.00	C
ATOM	173	3H1	7 C5	P	0	6.509	-1.340	-1.735	1.00	0.00	H
ATOM	174	4H1	7 C5	P	0	7.519	-1.102	-3.192	1.00	0.00	H
ATOM	175	5H1	7 C5	P	0	6.683	0.277	-2.430	1.00	0.00	H

Coordination file of polyNAGA10 in the GROMACS file format

1MEI	C1	1	1.438	2.218	2.396
1MEI	H11	2	1.331	2.229	2.383
1MEI	H12	3	1.457	2.117	2.434
1MEI	H13	4	1.482	2.224	2.297
2PCI	C1	5	1.644	2.304	2.527
2PCI	H11	6	1.651	2.216	2.591
2PCI	H12	7	1.678	2.386	2.590
2PCI	C2	8	1.495	2.326	2.491
2PCI	H21	9	1.484	2.423	2.441
2PCI	C3	10	1.413	2.332	2.621
2PCI	O1	11	1.362	2.230	2.667
2PCI	N1	12	1.403	2.452	2.681
2PCI	H1	13	1.447	2.531	2.636
2PCI	C4	14	1.340	2.476	2.811
2PCI	H41	15	1.415	2.523	2.876
2PCI	H42	16	1.310	2.384	2.861
2PCI	C5	17	1.219	2.569	2.799
2PCI	O2	18	1.229	2.688	2.828
2PCI	N2	19	1.105	2.514	2.756
2PCI	H2	20	1.022	2.570	2.747
2PCI	H3	21	1.102	2.415	2.733
3PCI	C1	22	1.892	2.268	2.463
3PCI	H11	23	1.888	2.207	2.553
3PCI	H12	24	1.930	2.364	2.498
3PCI	C2	25	1.745	2.282	2.411
3PCI	H21	26	1.717	2.184	2.373
3PCI	C3	27	1.727	2.378	2.291
3PCI	O1	28	1.700	2.328	2.182
3PCI	N1	29	1.740	2.511	2.302
3PCI	H1	30	1.723	2.563	2.216
3PCI	C4	31	1.780	2.594	2.415
3PCI	H41	32	1.802	2.538	2.505
3PCI	H42	33	1.696	2.660	2.440

3PCI	C5	34	1.902	2.682	2.383
3PCI	O2	35	1.925	2.781	2.452
3PCI	N2	36	1.981	2.646	2.282
3PCI	H2	37	1.960	2.564	2.227
3PCI	H3	38	2.063	2.702	2.259
4PCI	C1	39	2.061	2.301	2.266
4PCI	H11	40	2.111	2.380	2.322
4PCI	H12	41	1.980	2.350	2.214
4PCI	C2	42	2.001	2.204	2.371
4PCI	H21	43	2.084	2.185	2.439
4PCI	C3	44	1.961	2.064	2.321
4PCI	O1	45	2.003	1.966	2.383
4PCI	N1	46	1.879	2.054	2.216
4PCI	H1	47	1.847	2.138	2.171
4PCI	C4	48	1.831	1.927	2.162
4PCI	H41	49	1.884	1.841	2.201
4PCI	H42	50	1.849	1.927	2.054
4PCI	C5	51	1.681	1.911	2.188
4PCI	O2	52	1.599	1.937	2.100
4PCI	N2	53	1.646	1.869	2.310
4PCI	H2	54	1.717	1.848	2.378
4PCI	H3	55	1.548	1.856	2.332
5PCI	C1	56	2.272	2.154	2.210
5PCI	H11	57	2.239	2.102	2.299
5PCI	H12	58	2.357	2.213	2.244
5PCI	C2	59	2.160	2.248	2.157
5PCI	H21	60	2.099	2.191	2.087
5PCI	C3	61	2.215	2.369	2.077
5PCI	O1	62	2.144	2.468	2.059
5PCI	N1	63	2.340	2.361	2.027
5PCI	H1	64	2.392	2.276	2.043
5PCI	C4	65	2.413	2.471	1.965
5PCI	H41	66	2.511	2.478	2.013
5PCI	H42	67	2.364	2.568	1.981
5PCI	C5	68	2.433	2.446	1.816
5PCI	O2	69	2.515	2.362	1.777
5PCI	N2	70	2.359	2.518	1.731
5PCI	H2	71	2.369	2.505	1.632
5PCI	H3	72	2.293	2.586	1.768
6PCI	C1	73	2.232	1.916	2.114
6PCI	H11	74	2.128	1.946	2.099
6PCI	H12	75	2.234	1.879	2.216
6PCI	C2	76	2.317	2.047	2.105
6PCI	H21	77	2.292	2.090	2.008
6PCI	C3	78	2.469	2.027	2.095

6PCI	O1	79	2.524	2.045	1.986
6PCI	N1	80	2.544	1.994	2.202
6PCI	H1	81	2.644	1.987	2.185
6PCI	C4	82	2.504	1.957	2.337
6PCI	H41	83	2.396	1.954	2.350
6PCI	H42	84	2.542	2.033	2.406
6PCI	C5	85	2.564	1.822	2.374
6PCI	O2	86	2.686	1.804	2.371
6PCI	N2	87	2.479	1.725	2.410
6PCI	H2	88	2.379	1.743	2.410
6PCI	H3	89	2.514	1.634	2.434
7PCI	C1	90	2.270	1.833	1.865
7PCI	H11	91	2.363	1.795	1.822
7PCI	H12	92	2.279	1.940	1.851
7PCI	C2	93	2.258	1.798	2.017
7PCI	H21	94	2.165	1.741	2.027
7PCI	C3	95	2.361	1.696	2.070
7PCI	O1	96	2.328	1.621	2.162
7PCI	N1	97	2.483	1.693	2.015
7PCI	H1	98	2.502	1.757	1.939
7PCI	C4	99	2.592	1.603	2.053
7PCI	H41	100	2.568	1.546	2.142
7PCI	H42	101	2.678	1.665	2.079
7PCI	C5	102	2.635	1.506	1.942
7PCI	O2	103	2.725	1.426	1.963
7PCI	N2	104	2.571	1.510	1.824
7PCI	H2	105	2.597	1.446	1.750
7PCI	H3	106	2.496	1.576	1.810
8PCI	C1	107	2.027	1.868	1.795
8PCI	H11	108	2.060	1.971	1.803
8PCI	H12	109	1.990	1.844	1.895
8PCI	C2	110	2.155	1.781	1.774
8PCI	H21	111	2.189	1.798	1.673
8PCI	C3	112	2.137	1.628	1.789
8PCI	O1	113	2.237	1.556	1.785
8PCI	N1	114	2.014	1.579	1.807
8PCI	H1	115	1.937	1.645	1.806
8PCI	C4	116	1.980	1.443	1.846
8PCI	H41	117	2.068	1.388	1.882
8PCI	H42	118	1.941	1.388	1.760
8PCI	C5	119	1.877	1.446	1.959
8PCI	O2	120	1.909	1.480	2.073
8PCI	N2	121	1.751	1.413	1.927
8PCI	H2	122	1.729	1.387	1.832
8PCI	H3	123	1.679	1.414	1.998

9PCI	C1	124	1.922	1.944	1.561
9PCI	H11	125	1.996	2.021	1.579
9PCI	H12	126	1.830	1.999	1.544
9PCI	C2	127	1.910	1.860	1.692
9PCI	H21	128	1.904	1.756	1.661
9PCI	C3	129	1.776	1.887	1.764
9PCI	O1	130	1.695	1.795	1.774
9PCI	N1	131	1.747	2.008	1.818
9PCI	H1	132	1.657	2.016	1.863
9PCI	C4	133	1.829	2.129	1.824
9PCI	H41	134	1.918	2.122	1.762
9PCI	H42	135	1.863	2.143	1.927
9PCI	C5	136	1.754	2.253	1.775
9PCI	O2	137	1.730	2.268	1.656
9PCI	N2	138	1.722	2.345	1.867
9PCI	H2	139	1.746	2.330	1.964
9PCI	H3	140	1.674	2.429	1.838
10PCI	C1	141	1.845	1.787	1.356
10PCI	H11	142	1.889	1.732	1.273
10PCI	H12	143	1.780	1.859	1.307
10PCI	C2	144	1.956	1.872	1.426
10PCI	H21	145	1.965	1.954	1.355
10PCI	C3	146	2.096	1.809	1.424
10PCI	O1	147	2.108	1.687	1.433
10PCI	N1	148	2.206	1.885	1.409
10PCI	H1	149	2.294	1.836	1.406
10PCI	C4	150	2.219	2.031	1.400
10PCI	H41	151	2.124	2.084	1.403
10PCI	H42	152	2.264	2.055	1.304
10PCI	C5	153	2.308	2.088	1.511
10PCI	O2	154	2.370	2.014	1.589
10PCI	N2	155	2.315	2.221	1.519
10PCI	H2	156	2.372	2.264	1.591
10PCI	H3	157	2.263	2.278	1.455
11PEE	C1	158	1.623	1.662	1.355
11PEE	H11	159	1.556	1.596	1.410
11PEE	H12	160	1.647	1.613	1.260
11PEE	H13	161	1.567	1.753	1.332
11PEE	C2	162	1.750	1.694	1.435
11PEE	H21	163	1.715	1.750	1.522
11PEE	C3	164	1.810	1.562	1.487
11PEE	O1	165	1.782	1.526	1.601
11PEE	N1	166	1.883	1.487	1.403
11PEE	H1	167	1.900	1.523	1.310
11PEE	C4	168	1.937	1.355	1.433

11PEE	H41	169	1.889	1.282	1.368
11PEE	H42	170	1.915	1.324	1.535
11PEE	C5	171	2.089	1.347	1.414
11PEE	O2	172	2.135	1.292	1.314
11PEE	N2	173	2.166	1.399	1.509
11PEE	H2	174	2.266	1.395	1.500
11PEE	H3	175	2.124	1.444	1.589

GROMACS energy minimization file

title	fws
cpp	/usr/bin/cpp
define	-DFLEXIBLE
constraints	none
integrator	steep
dt	0.1
nsteps	4000
nstlist	10
ns-type	grid
rlist	1.0
coulombtype	PME
rcoulomb	1.0
vdwtype	cut-off
rvdw	1.4
fourierspacing	0.12
emtol	100.0
emstep	0.01

Table 3: Energy minimization parameters

GROMACS molecular dynamics simulation parameters file

title	Production Simulation
cpp	/lib/cpp
integrator	md
dt	0.001
nsteps	50000000
nstxout	500000
nstvout	500000
nstfout	500000
nstlog	500000
nstenergy	500000
nstxtcout	500000
xtc_precision	500000
xtc-grps	System
energygrps	System
nstlist	10
ns-type	grid
pbc	xyz
rlist	1.2
coulombtype	PME
rcoulomb	1.2
fourierspacing	0.12
vdw-type	Cut-off
rvdw	1.2
tcoupl	nose-hoover
tc-grps	system
tau_t	0.2
ref_t	360
Pcoupl	Parrinello-Rahman
Pcoupltype	Isotropic
tau_p	1.0
compressibility	4.5e-5
ref_p	1.0
gen_vel	yes

gen_temp	360
gen_seed	9999
constraints	none

TABLE 4: Molecular Dynamics simulation parameters